ABSTRACT

Title of Document: BUILDING BLOCK APPROACH TO THE SYNTHESIS OF A CUCURBIT[7]URIL DERIVATIVE BEARING SULFONATE FUNCTIONAL GROUPS

Lorene E. Brownlow, Master of Science, 2014

Directed By: Professor, Lyle Isaacs
Department of Chemistry and Biochemistry

Low aqueous solubility prevents 40-70% of new pharmaceutical agents from reaching their full potential. The use of molecular containers as solubilizing agents is one solution currently under development. Chapter 1 introduces molecular containers under investigation as drug delivery excipients. Synthetic approaches, properties and important derivatives of cyclodextrins and cucurbiturils are briefly reviewed. Chapter 2 describes the tested hypothesis that the addition of sulfonate functional groups to CB[7] will enhance the aqueous solubility of the CB[7] derivative as compared to CB[7] itself. The building-block approach to obtain a difunctionalized CB[7] derivative by the condensation of glycoluril hexamer (**21**) and $((CH_2)_4SO_3Na)_2$ glycoluril bis(cyclic ether) (**30**) is described. The new CB[7] derivative had surprisingly low aqueous solubility (20.2 mM), but very similar molecular recognition properties to those of CB[7]. The CB[7] derivative was investigated for its use as an excipient for drug solubilization and found to have no enhancement compared to CB[7].

BUILDING BLOCK APPROACH TO THE SYNTHESIS OF A CUCURBIT[7]URIL DERIVATIVE BEARING SULFONATE FUNCTIONAL GROUPS

By

Lorene E. Brownlow

Thesis submitted to the Faculty of the Graduate School of the
University of Maryland, College Park, in partial fulfillment
of the requirements for the degree of
Master of Science
2014

Advisory Committee:
Professor Lyle Isaacs, Chair
Professor Jeffery Davis
Professor Philip DeShong

Dedication

To my parents Cristie Taffin and Robert Brownlow,
and to my husband Alex.

Acknowledgements

I would like to thank my advisor Professor Lyle Isaacs for all of the time and effort you have dedicated to guiding me through my graduate career. I am thankful for the knowledge you have passed on to me. Thank you for your assistance in all of my research ventures, making this thesis possible.

I wish to express my sincere gratitude to Dr. Michael Montague-Smith. Working with you as a Teaching Assistant was a truly enjoyable experience. Your guidance in and outside of the classroom has proven to be invaluable.

I would like to thank two undergraduate professors of mine, Professors Martin Jones and Robert Astalos. Thank you Professor Martin Jones, your love for organic chemistry ignited a desire in me to pursue a higher degree in the same field. Thank you Professor Robert Astalos, your passion for physics inspired me to pursue knowledge of all things.

I would like to thank former Isaacs group member Dr. James Wittenberg. Thank you for teaching me many essential laboratory techniques. I was able to learn so much due to your patience and ability to communicate the concepts in great detail. Thank you for your help not only as a lab mate, but also as a friend.

I would also like to thank the current Isaacs group members. You have made the time spent in lab not only productive, but incredibly delightful as well. Thank you for your input and helpful suggestions. A special thank you to Dr. Liping Cao for your instruction and to Brittany Vinciguerra for your knowledge, support, and friendship.

Finally, I would like to thank my parents, Robert and Melissa Brownlow and Mark and Cristie Taffin, my husband Alex Robinson, and my siblings. I could not have done it without all of the support, encouragement, and understanding given to me throughout my pursuit of higher education.

Table of Contents

List of Schemes

Chapter 1

Chapter 2

List of Charts

Chapter 1

Chapter 2

List of Figures

Chapter 1

Chapter 2

List of Abbreviations

1°	primary
2°	secondary
Å	angstrom
α	alpha
β	beta
γ	gamma
μM	micromolar
ATR	attenuated total reflectance
CB[*n*]	cucurbit[*n*]uril
CD	cyclodextrin
$CHCl_3$	chloroform
cm	centimeter
cm^{-1}	wavenumber
d	doublet
D_2O	deuterium oxide
CH_2Cl_2	dichloromethane
$Cl(CH_2)_3I$	1-chloro-3-iodopropane
Cy	cyclohexyl
DCl	deuterium chloride
DMF	dimethylformamide
DMSO	dimethylsulfoxide
ESI-MS	electrospray ionization-mass spectrometry

Et_2O	ethylether
EtOH	ethanol
equiv	equivalents
g	gram
HR-MS	high-resolution mass-spectrometry
h	hour
HCl	hydrochloric acid
Hg	mercury
H_2O	water
H_2SO_4	sulfuric acid
Hz	hertz
K	kelvin
K_a	equilibrium association constant
KCl	potassium chloride
$K_2S_2O_8$	potassium persulfate
IR	infrared
J	coupling constant
KBr	potassium bromide
LDA	lithium diisopropylamide
m	multiplet
M	molar
M^+	molecular ion
Me	methyl

MeOH	methanol
$MeSO_3H$	methanesulfonic acid
$MgSO_4$	magnesium sulfate
MHz	megahertz
min	minute
mL	milliliter
mM	millimolar
M.p.	melting point
m/z	mass to charge ratio
N_2	nitrogen gas
NaH	sodium hydride
$NaHCO_3$	sodium bicarbonate
NaOH	sodium hydroxide
Na_2SO_3	sodium sulfite
$(NH_4)_2S_2O_8$	ammonium persulfate
NMR	nuclear magnetic resonance
OH	hydroxyl
p	*para*
ppm	parts per million
rpm	rotations per minute
RT	room temperature
s	singlet
SBE	sulfobutyl ether

t	triplet
TFA	trifluoroacetic acid
THF	tetrahydrofuran
$TiCl_4$	titanium(IV) chloride

Chapter 1: Molecular Containers

1.1 Introduction to Molecular Containers

Solubility issues often overshadow the excitement of discovering a new compound with pharmaceutical activity. Approximately 40-70% of new pharmaceutical agents fall into the Biopharmaceutics Classification System Class II.[1] These compounds exhibit the high intestinal permeability required for a successful pharmaceutical agent, but suffer from low aqueous solubility. This limitation has led researchers to devote significant resources to the discovery of methods to enhance the solubility of these potential pharmaceuticals. One solution with great promise is the use of molecular containers as excipients.

Molecular containers are an interesting group of compounds that are able to recognize and associate with another molecule through non-covalent interactions. The strength of the association is based on the strength of intermolecular interactions such as hydrogen bonding, ion-dipole, dipole-dipole, π-π, metal coordination, the hydrophobic effect and van der Waals forces. The field of supramolecular chemistry has greatly expanded with the discovery of different families of molecular containers as well as their innumerable applications. This chapter will focus on two families of molecular containers (cyclodextrins and cucurbiturils) that are currently under investigation for their use as excipients for drug solubilization.

1.2 Cyclodextrins: A family of bowl-shaped molecular containers

Cyclodextrins (CDs) are cyclic oligosaccharides composed of α-D-glucose units linked by α-1,4 glycosidic bonds that are obtained by enzymatic degradation of starch. They first appeared in literature in 1891 when Villiers and co-workers noticed that along with reducing dextrins a small amount of crystalline material was obtained from starch digestion of *Bacilus amylobacter*.[2] By 1935 the more prevalent CDs (6-8 α-D-glucose units per macrocycle) known as α-, β-, and γ-CD were isolated.[3] Interestingly, it took an additional 14 years for all three structures to be determined by x-ray crystallography (Chart I-1).[4] The identified bowl-like structure makes them compelling molecular containers.

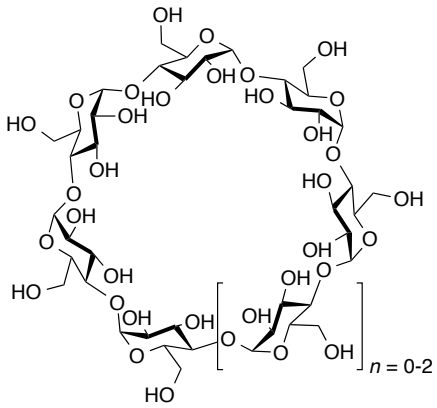

Chart I-1. Chemical structures of α-, β-, and γ-CD.

The unique structure of CDs controls their properties. They have two rims of different sizes that are flanked with hydroxyl groups. These hydroxyl groups are advantageous in two ways: their hydrophilic nature increases the water solubility of the macrocycle (α-CD: 149 mM, β-CD: 16 mM, γ-CD: 178 mM)[5] and are able to form hydrogen bonds with appropriate guests. Hydrogens and ether-like oxygens point inward which produces an apolar environment causing the cavity to be more hydrophobic in

nature. These features, when combined, make CDs able to act as molecular containers for alkyl and aryl residues especially if they contain motifs able to hydrogen bond with one of the hydroxyl groups of one of the rims.

Complexation between a CD and a guest is the result of a complicated equilibrium. In fact, a combination of energetically favorable interactions is required for complexation to occur. Dissolution of CDs in aqueous media results in water molecules encompassing the apolar cavity that gives rise to a highly energetic, highly ordered water molecule arrangement.[5] Therefore it is thermodynamically favorable to displace the water molecules with an alkyl or aryl guest molecule. Another contributing factor is the increase in van der Waals interactions between the apolar cavity and guest. Hydrogen bonding between a guest and a hydroxyl group on one of the rims can also aid in complexation. The combination of these interactions makes complexation a thermodynamically favorable process.

The glycosidic linkages between the individual sugar units of the CD macrocycles make the bowl-like structure fairly flexible. This flexibility makes the cavity able to bind a wide variety of guests. A single β-CD can form a host•guest complex with molecules ranging from 1-propanol (**4**) to protriptyline (**5**) (Chart I-2).[6] Not surprisingly, the strength of the complex is dependent on favorable electrostatic interactions as well as hydrogen bonding between the guest and the CD hydroxyl rim. Naphthalene (**6**) association with β-CD, $K_a = 6.7 \times 10^2\ M^{-1}$, is a result of the hydrophobic effect while 1-naphthalene acetate (**7**) forms a much stronger complex with $K_a = 2.2 \times 10^4\ M^{-1}$ because of hydrogen bonding as well as the hydrophobic effect.[7,8] This dependence on hydrogen bonding makes CD•guest complexation stimuli-responsive. A change in pH from 8.2 to

1.6 results in a slight increase in K_a from 2.3×10^2 to 4.3×10^2 M^{-1} for *trans*-3-hydroxycinnamate (**8**) with β-CD in aqueous solution.[9] The K_a for many CD•guest complexes are dependent on changes in the pH of the solution.

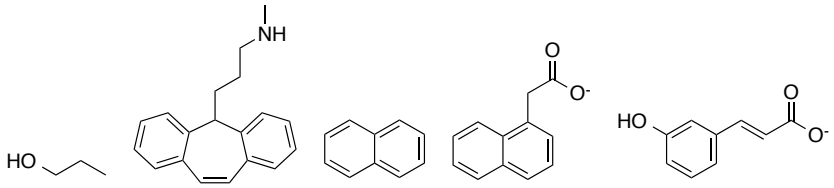

Chart I-2. Chemical structures for β-CD guests (1-propanol (**4**), protriptyline (**5**), napththalene (**6**), 1-naphthalene acetate (**7**), *trans*-3-hydroxycinnamate (**8**)).

The ease of derivitization of the 1° and 2° hydroxyl groups along the rims of the CD's have allowed for many derivatives to be synthesized. One example of a CD derivative currently being employed as a drug delivery excipient is Captisol™. Captisol™ (also known as SBE7-β-CD where 7 refers to the average degree of substitution) is a derivative of β-CD with an average of 7 sulfobutyl ether sodium salt arms variably substituted along the rims.[10] The anionic CD has highly enhanced water solubility (>500 mM)[11] and has been shown to form highly soluble host•guest complexes with a wide variety of pharmaceuticals (i.e. indomethacin (**9**), thiabendazole (**10**), naproxen (**11**), and cinnarizine (**12**) (Chart I-3). Although CDs suffer from relatively low K_a's and poor selectivity, they have been proven to be useful molecular containers for drug solubility enhancement for drug delivery.

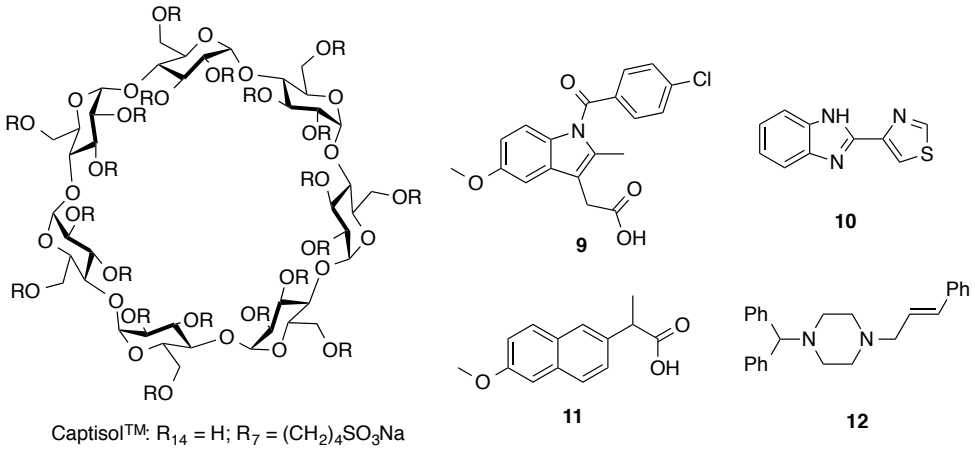

Chart I-3. Chemical structures for Captisol™ and insoluble drugs (indomethacin (**9**), thiabendazole (**10**), naproxen (**11**), and cinnarizine (**12**)).

1.3 Cucurbiturils: A family of open-ended barrel-like molecular containers

1.3.1 Introduction to Cucurbiturils

In 1905, Behrend and co-workers reported that the condensation reaction between glycoluril and two equivalents of formaldehyde in concentrated hydrochloric acid delivered a compound now known as Behrend's polymer.[12] Little was known about Behrend's polymer other than its dissolution in hot sulfuric acid, upon which the addition of cold water would lead to a new substance as a crystalline precipitate. Unfortunately, the limited instrumentation techniques of that time prevented full characterization. Behrend's results were not revisited until 1981, over 75 years after the initial publication, when Mock and co-workers repeated Behrend's experiment. The crystalline precipitate was collected and characterized (Scheme I-1).[13] The IR suggested the preservation of the glycoluril subunits (1720 cm^{-1}, KBr). The presence of only three signals of equivalent intensity in the ^{1}H NMR indicated a molecule with very high symmetry. X-ray crystallography was used to determine the structure of a complex formed between the precipitate and calcium bisulfate. Mock reported the characterization of the interesting

precipitate under the name cucurbituril (later referred to as cucurbit[6]uril) based on the resemblance of the structure to a pumpkin (family Cucurbitaceae).

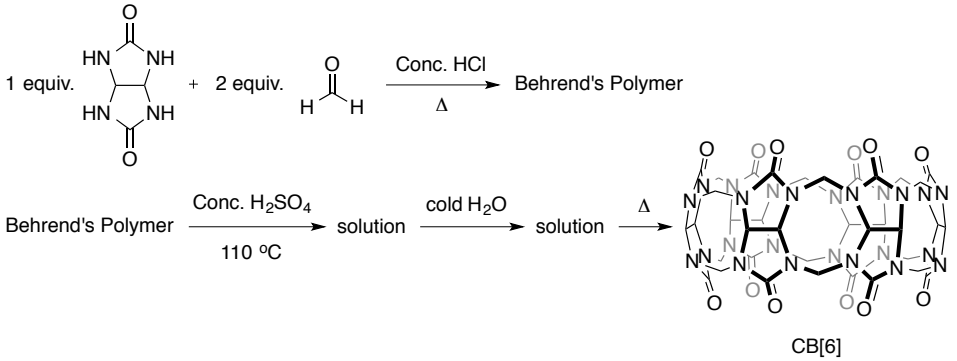

Scheme I-1. Glycoluril condensation reaction to form Behrend's polymer and the transformation to CB[6].

By performing the reaction under milder kinetically controlled conditions, Day and Kim independently expanded the cucurbit[*n*]uril (CB[*n*]) family by the isolation of additional CB[*n*] (*n* = 5-8), where *n* represents the number of glycoluril units in the macrocycle (Scheme I-2).[14,15] Isaacs reported the isolation of the largest CB[*n*] macrocycle, CB[10], in 2005.[16] The isolation of these different macrocycles allowed the unique properties of the CB[*n*] homologues to be fully investigated.

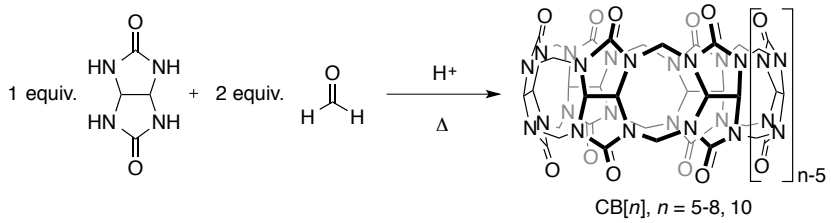

Scheme I-2. Glycoluril condensation reaction to form CB[*n*].

The solubility of the CB[*n*] homologues is dependent on the ability of the macrocycles to self-associate in the crystalline state.[17] The strength of the association is affected by the number of inter-cucurbituril CH---O interactions between the equatorial methine protons and the ureidyl carbonyl portal of a neighboring CB[*n*]. Interestingly, the CB[*n*] homologues with an even number of glycoluril units are able to form more CH---O

interactions. This efficient crystal packing provides an explanation for the observed low aqueous solubility of CB[6], CB[8], and CB[10] (< 20 μM). The CB[*n*] homologues with an odd number of glycoluril units, CB[5] and CB[7], have less efficient crystal packing and moderate solubilities (20-30 mM). An aqueous solubility enhancement is observed for all CB[*n*] homologues under acidic conditions or in the presence of certain cations due to the interactions between the electrostatically negative ureidyl carbonyl portals of a CB[*n*] and the positively charged ion (i.e. alkali metals, alkyl and aryl ammonium ions). This ability to capture a guest molecule inside the cavity makes the CB[*n*] homologues compelling compounds.

Many interactions affect the ability of a CB[*n*] to strongly bind a specific guest. Each CB[*n*] has a fairly rigid structure resulting in a level of selectivity not seen in previous molecular containers. Favorable electrostatic interactions play a large role in CB[*n*]•guest binding. The carbonyl portals and hydrophobic cavity make CB[*n*] ideal hosts for hydrophobic and cationic guests in water by hydrogen-bonding, ion-dipole interactions, and the hydrophobic effect. The varying cavity sizes of the CB[*n*] allow for each macrocycle to interact with a set of guests based on their size. Upon solubilization, the cavity is filled with high-energy water molecules that can be displaced by an appropriate guest. Strong host•guest complexes can form between a CB[*n*] and guests of appropriate size that are able to interact with one or both carbonyl portals, such as alkyl and aryl diammonium ions (Scheme I-3).[18]

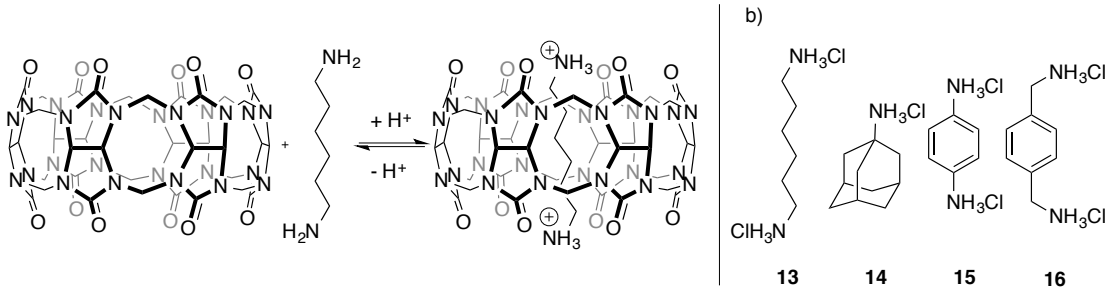

Scheme I-3. a) Equilibrium of complexation between hexanediamine and CB[6]. b) Ammonium guests of various sizes and positive charges able to interact with CB[*n*] (hexanediamine•2HCl (**13**), adamantane amine•HCl (**14**), *p*-phenylenediamine•2HCl (**15**), *p*-xylenediamine•2HCl (**16**)).

The formation of a complex is highly dependent on favorable electrostatic interactions between positively charged ammonium ions and the carbonyl portal. The binding interactions are less favorable if the ammonium ion is deprotonated and the strength of the complex will decrease by up to 4 orders of magnitude. This decrease often will result in guest dissociation. Excitingly, this dependence on electrostatic interactions makes the binding responsive to stimuli, such as pH. The hydrogen-bond between the carbonyl of the CB[*n*] and the diammonium ion stabilizes the charge, which can result in a pK_a shift in many cases. Nau and co-workers reported a pK_a shift of +4.0 for thiabendazole **10** upon complexation with CB[7].[19] The large pK_a shift allows for complexation at higher pH's, making CB[*n*] ideal molecular containers to bind and stabilize certain compounds at pH values not possible for the free compound. These unique properties have led to many exciting advances in CB[*n*]-assisted drug delivery.

The strength of the host•guest complex is highly dependent on the fit of the guest inside the cavity, making guests of different sizes ideal for binding to each of the CB[*n*]. The association equilibrium constant K_a has been determined for many host•guest complexes in a 50 mM sodium acetate buffer.[20] The hexanediammonium ion (**13**) is the ideal size for CB[6] complexation with $K_a = 4.49 \times 10^8\ M^{-1}$. The larger CB[7] cavity has

lower affinity for **13**, $K_a = 8.87 \times 10^7$ M^{-1}, but is perfect for the larger carbon skeleton of the adamantane ammonium ion (**14**) with $K_a = 4.23 \times 10^{12}$ M^{-1}. Not surprisingly, the strongest complexes will form when there is an ideal match between the size of the cavity and the size of the guest.

The high water solubility (as compared to CB[6] and CB[8]), ideal cavity size, and reversible binding of CB[7] have made it the most widely studied CB[*n*] homologue. These specific characteristics give it potential as a molecular container for drug delivery (Chart I-4). Albendazole (**17**), an anti-parasitic drug with potential anti-cancer properties, has poor aqueous solubility (0.03 mM) at a neutral pH.[21] A significant solubility enhancement to 7.1 mM (>200-fold) was obtained in a 10 mM solution of CB[7].[21] The anti-cancer drug camptothecin (**18**), is insoluble in water at pH = 7.4 and is only slightly soluble at pH = 2 (0.0595 mM).[22] In the presence of a 7.6 mM CB[7] solution at pH = 2.0, however, the water solubility is enhanced to 4 mM (67-fold). These impressive solubility enhancements show great promise for the use of CB[*n*] as a solubilizing excipient for the purpose of drug delivery.

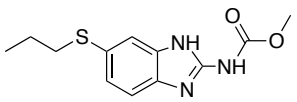

17

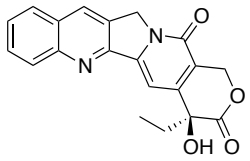

18

Chart I-4. Structures of the insoluble drugs (albendazole (**17**) and camptothecin (**18**)).

1.3.2 Functionalized Cucurbiturils

The low solubility of the CB[*n*] (*n* = 6, 8, 10) homologues places an unfortunate limit on their widespread application. This limitation has led research groups to investigate synthetic routes to functionalized CB[*n*] derivatives with enhanced solubility

in aqueous and organic solvents. In 2003, Kim and co-workers reported the (per)hydroxylation of pre-formed CB[*n*] macrocycles with varied success (42, 45, 5, and 4% yields for *n* = 5-8, respectively).[23] $(OH)_{12}$CB[6], which was obtained in the best yield, was further investigated and found to be soluble in organic solvents such as DMSO and DMF. The reactivity of the hydroxyl functional group allowed for additional derivitization reactions (Scheme I-6 (a)). These compelling CB[*n*] derivatives lend themselves to covalent attachments to glass and silica surfaces, allowing for the combination of the microscopic binding properties of CB[*n*] with macroscopic techniques such as chromatography. A mono-substituted CB[*n*] derivative was reported in 2012, when Scherman and co-workers tamed the hydroxylation reaction.[24] They were able to isolate $(OH)_1$CB[6], which could also be further functionalized. These mono functionalized CB[6] derivatives are ideal for highly controlled, single point attachment which greatly broadens their potential applications (Scheme I-6 (b)). However, these synthetic routes are limited to the smaller CB[5-6] macrocycles, which still leaves a void of routes to functionalized CB[7] macrocycles able to bind more interesting guests in the larger cavity.

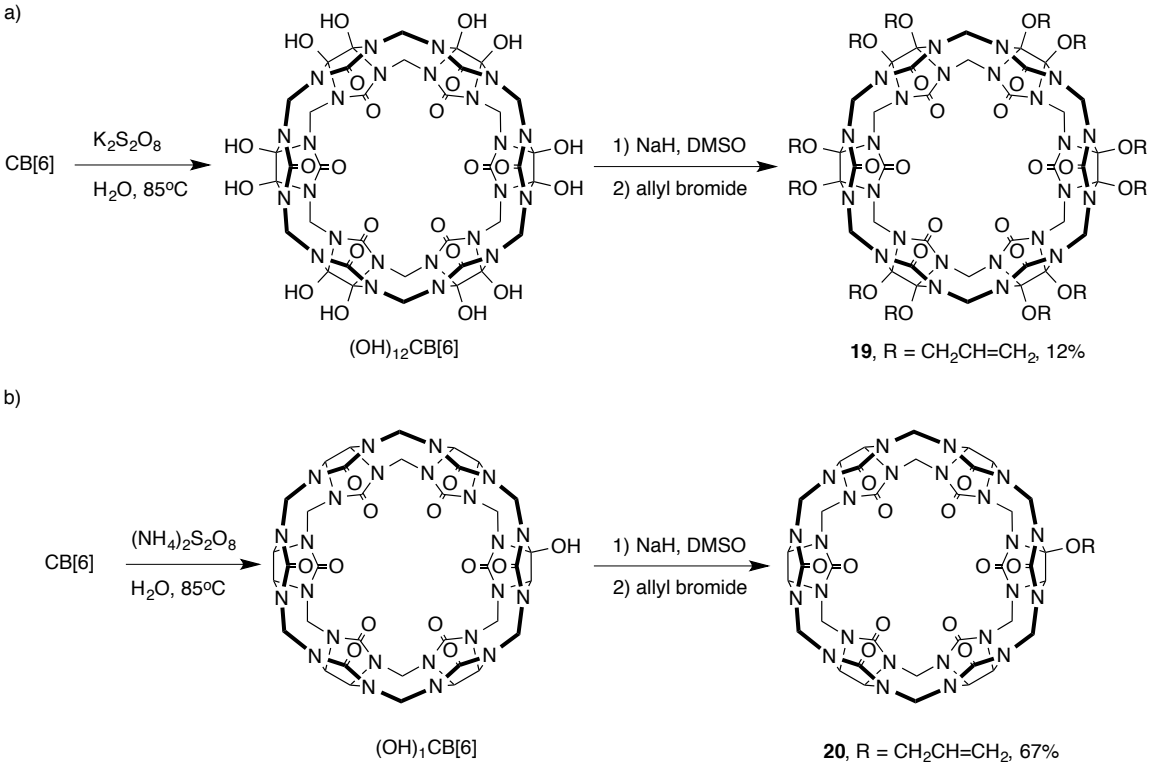

Scheme I-6. Synthesis of functionalized CB[6] derivatives.[23,24]

1.3.3 The Building-Block Approach to Functionalized CB[7]

A facile route to CB[7] derivatives was realized by Isaacs and co-workers. The essential mechanistic understanding of CB[*n*] formation provided by Isaacs led to the exciting large-scale synthesis of an important synthetic intermediate. In 2011, they reported the templated synthesis of acyclic glycoluril hexamer (**21**) on the gram scale (Scheme I-7 (a)).[25] Compound **21** was then combined with a functionalized glycoluril bis(cyclic ether) (**22**) to yield a functionalized CB[7]. Isaacs and co-workers reported a family of alkylated CB[7] derivatives in 2012 (Scheme I-7 (b)).[26] The addition of the bulky R groups on the CB[7] derivatives results in incredibly enhanced water solubilities, Me_2CB[7] (≥264 mM) and CyCB[7] (≥181 mM) which are likely due to interference with their ability to form inter-cucurbituril CH---O interactions in the solid state. The molecular recognition properties of the alkylated CB[7] derivatives were also

investigated and found to be comparable to those of their CB[7] counterpart. Fortunately, the alkyl groups were found to enhance the water solubility without affecting the molecular recognition of the macrocycles.

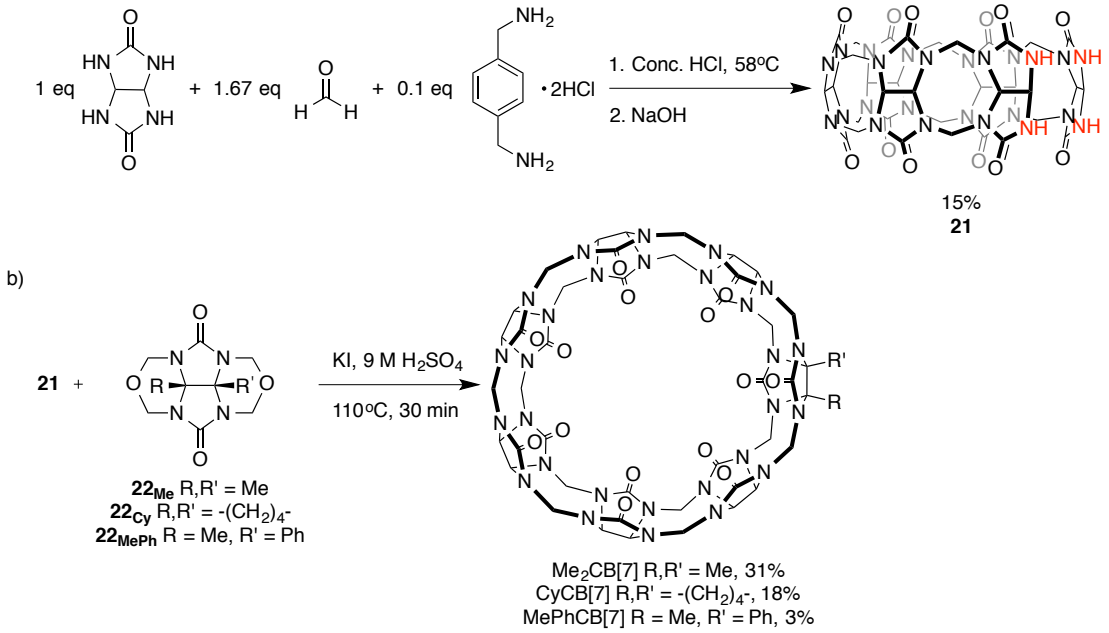

Scheme I-7. a) Templated synthesis of acyclic glycoluril hexamer (**21**). b) Synthesis of alkylated CB[7] derivatives.

The enhanced water solubility and expected molecular recognition of Me_2CB[7] led to the investigation of its use as a molecular container for the previously studied albendazole (**17**) (Figure I-1).[26] In a 0.01 M DCl solution in D_2O at pD = 2, Me_2CB[7] performed the same as CB[7] at lower concentrations of host (0-10 mM). Surprisingly, a 15 mM Me_2CB[7] solution was only able to enhance the solubility of **17** to 5.8 mM while a CB[7] solution of the same concentration was able to solubilize 1.4 times the amount of **17** (8.1 mM). Even solutions with very high concentrations of Me_2CB[7] (up to 50 mM) were unable to enhance the solubility of **17** past ~ 6 mM. This unexpected limitation led to the conclusion that the methyl groups are able to enhance the solubility of the free host by disrupting the crystal packing, but when paired with a guest occupying the carbonyl

portals, the alkyl groups then act to hinder the solubility of the CB[7]•**17** complex. Therefore, the design of a suitable excipient for drug delivery must include functional groups able to enhance the water solubility beyond simply disrupting the crystal packing in order to obtain a soluble host•guest complex.

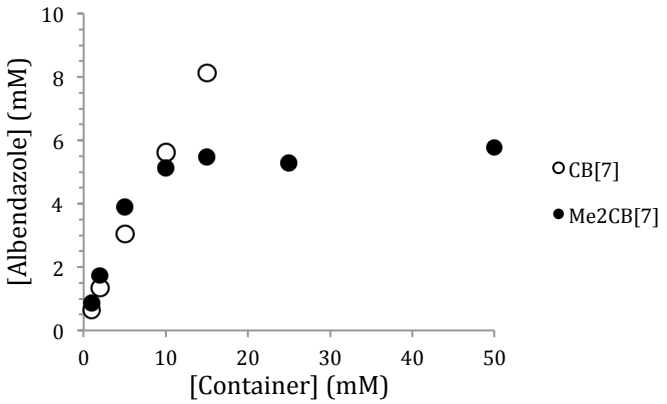

Figure I-1. Phase solubility diagram for albendazole (**17**) with hosts CB[7] and Me_2CB[7].

Chapter 2: Synthesis and Recognition Properties of a Cucurbit[7]uril Derivative Bearing Sulfonate Functional Groups

2.1 Introduction

It has been reported that the addition of sulfonate groups can be used to highly enhance the water solubility of molecular containers, i.e. Captisol™ (>500 mM) and an acyclic CB[*n*]-type molecular container (**23**) (346 mM), (Chart II-1).[27] Sulfonate functional groups are ideal due to their biocompatibility. They have very low pK_a's, allowing for consistent charge across the biologically relevant pH range. Sulfonate functional groups have also been shown to aid in the removal process through urine excretion. Accordingly, we hypothesized that a CB[7] derivative bearing sulfonate functionality might have high solubility on its own, as well as the host•guest complex with insoluble drugs and would therefore be a useful excipient for drug solubilization.

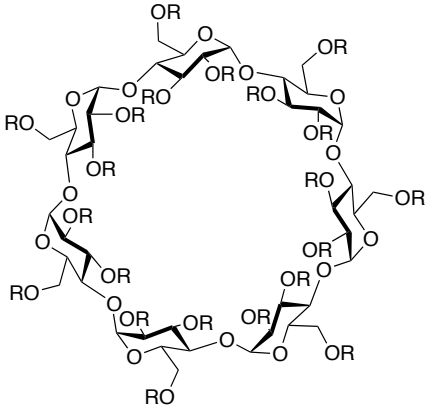

Captisol™: R_{14} = H; R_7 = $(CH_2)_4SO_3Na$

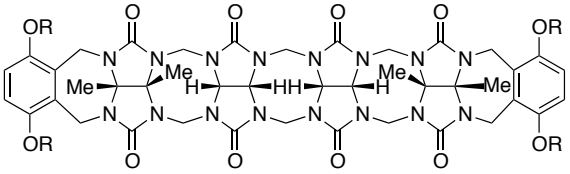

Acyclic CB[*n*]-type molecular container (**23**) R = $(CH_2)_3SO_3Na$

Chart II-1. Chemical structures of molecular containers bearing sulfonate functional groups: Captisol™ and an acyclic CB[*n*]-type molecular container (**23**).

We decided to use a functionalized bis(cyclic ether) synthetic route similar to the one employed by Isaacs and co-workers in 2012 (Scheme II-1).[26] First, we reacted

butanedione (**24**) with isopropylamine (**25**) in Et_2O with $TiCl_4$ as a catalyst to obtain the known diimine (**26**).[28] We then deprotonated **26** with 2.3 equiv. of LDA in THF which was followed by dialkylation with 1-chloro-3-iodopropane. Compound **27** was delivered in 75% yield after a hydrolytic workup (conditions: 1 M HCl (aq.) addition and CH_2Cl_2 extraction) followed by distillation. The functionalized glycoluril (**28**) was synthesized by the condensation reaction of urea and **27** in TFA and benzene at reflux (30% yield). A combination of **28** and formalin in HCl resulted in the formation of compound **29** (90% yield) which is an ideal S_N2 substrate for the introduction of the sulfonate functionality. Finally, **29** was treated with Na_2SO_3 in H_2O and converted, almost quantitatively, to compound **30** that was isolated in 50% yield.

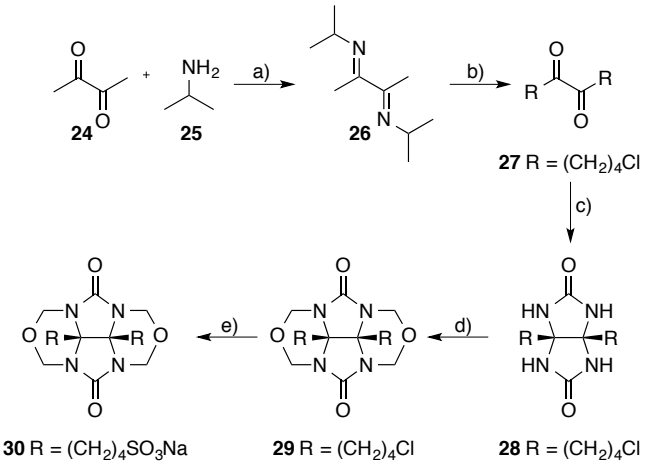

Scheme II-1. Synthesis of **30**. Conditions: (a) Et_2O, $TiCl_4$; (b) LDA, THF, $Cl(CH_2)_3I$, 75%; (c) urea, TFA, benzene, reflux, 30%; (d) formalin, HCl, 90%; (e) Na_2SO_3, H_2O, 50%.

2.2 Synthesis and Purification of Host 1

We used the unique building-block approach outlined by Isaacs and co-workers to obtain a CB[7] derivative with two identical alkyl chains bearing sulfonate functional groups by the condensation reaction between **30** and **21** (Scheme II-2). ^1H NMR spectroscopy with **16** was used to calculate the percent content of Host **1** in the crude

reaction mixture by integration of Host **1•16** Ar-H hydrogens of **16** at 6.60 (s, 4H) versus that of the methylene/methine C-H hydrogens of Host **1** at 5.35-5.80 (m, 26H). This procedure allowed us to determine the composition to be 46% Host **1**, 5% CB[6], 49% other (Appendix). The crude solid was then dissolved in H_2O (5 mL) and loaded onto a column (3 cm diameter × 50 cm long) containing 35 cm Dowex 50WX2 ion-exchange resin pretreated with H_2O and eluted with H_2O (600 mL). ^1H NMR spectroscopy, in the presence of **16**, was used to assess the fractional purity, and the appropriate fractions were combined. The solvent was removed under reduced pressure. The residue was dissolved in H_2O (10 mL) and subsequently precipitated in MeOH (40 mL). We collected the solid by centrifugation and subsequently suspended it in H_2O (5.0 mL). The solution was adjusted to pH = 7.0 using a hydroxide solution (0.5 M aq.) with the desired counter ion. The solvent was removed under reduced pressure and then dried further under high vacuum for 18 hours to give the product as a white solid, 28% yield.

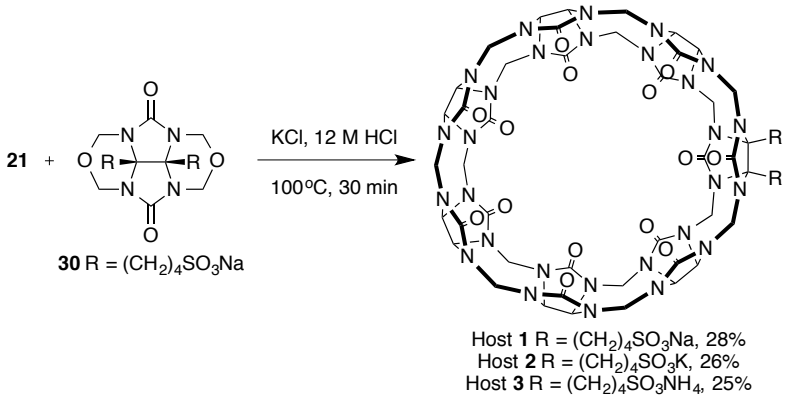

Scheme II-2. Synthesis of Hosts **1-3** by the condensation reaction between **21** and **30**.

2.3 Properties of Host 1

2.2.1 Characterization of Host 1

Host **1** was fully characterized by IR, ^{1}H NMR, ^{13}C NMR, ESI-MS, and HR-MS (see Appendix). As expected, the ^{1}H NMR confirms two equivalent $(CH_2)_4SO_3Na$ arms attached to the equatorial position of a glycoluril unit, which can be determined by the relative integrations of the signals (14:12:14:4:4:4:4) (Figure II-1 (b)). Also, the increased splitting of methylene/methine CH hydrogens on the CB[7] backbone indicates a loss of symmetry compared to the singlet and doublets of CB[7]. Upon the addition of **16** the upfield-shifted H-atoms of the diastereotopic methylene groups of Host **1** are resolved to three doublets of relative intensity 2, and one doublet of relative intensity 1 (Figure II-1 (a)). This change in the ^{1}H NMR spectra appearance upon the addition of **16** is consistent with the previously reported alkylated CB[7] derivatives.

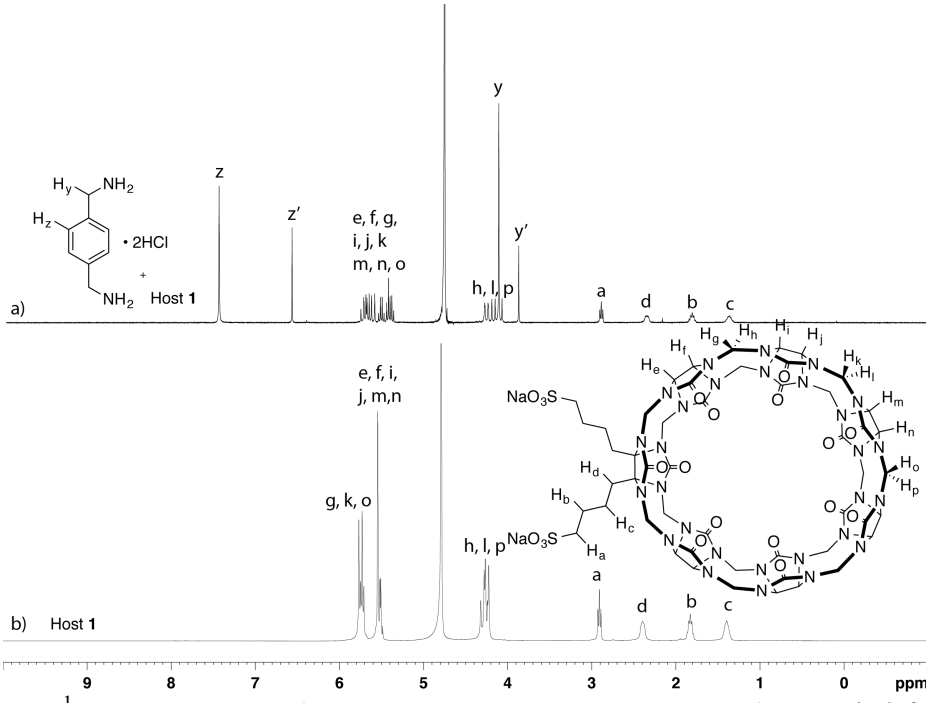

Figure II-1. ^{1}H NMR spectra (400 MHz, D_2O, room temperature) recorded for (a) 1:2 mixture Host **1** (1 mM) and **16** (2 mM) (b) Host **1** (1 mM).

2.2.2 Aqueous Solubility Properties of Hosts 1-3

Different counter-ions were investigated to measure their effect on the water solubility of the hosts bearing sulfonate functional groups. The ammonium counter-ion resulted in a disappointing 15.8 mM solution of Host **3**. Host **2** (K^+ counter-ion) resulted in a slightly better 17.2 mM solution. Surprisingly, the highest water solubility was found to be only 20.2 mM with the Na^+ counter-ion for Host **1**. The addition of the sulfonate groups did not enhance the aqueous solubility beyond that of CB[7] (20-30 mM) as expected. This unfortunate lack of aqueous solubility enhancement is likely due to the hydrophobic nature of the 8 CH_2 groups that are added along with the SO_3Na groups.

Container	hydroxide solution used to adjust pH	% yield	aqueous solubility (mM)
Host **1**	NaOH	28%	20.2
Host **2**	KOH	26%	17.2
Host **3**	NH_4OH	25%	15.8

2.2.3 X-Ray Crystal Structure of Host 1

We were fortunate to obtain single crystals of the Host **1•16** complex that were suitable for structure determination by x-ray crystallography. The structure of one of the Host **1•16** complexes indicates a structural similarity to CB[7] (Figure II-2 (a)).[14] The distance between the ureidyl C=O O-atoms of a single glycoluril unit of Host **1** averages 6.066 Å (range of 5.884-6.188 Å), comparable to 6.050 Å (range 5.913-6.114 Å) of CB[7]. Another similarity is the dimension along the equator of the hosts as seen by the distance between the opposing methine C-atoms on every fourth glycoluril: Host **1**

averages 11.596 Å (range 11.179-11.918 Å), CB[7] average 11.398 Å (range 11.247-11.516 Å). Another comparison can be made for the distance between the ureidyl C=O O-atoms on every fourth glycoluril of one portal, Host **1** averages 8.128 Å (range 7.152-9.042 Å, standard deviation = 0.746 Å) while CB[7] has an average distance of 8.139 Å (range 7.553-8.718 Å, standard deviation = 0.364 Å). The larger range and higher standard deviation attributed to Host **1** indicates the glycoluril units pivot slightly where one O-atom will shift inward while the other shifts outward, but only to a small extent. These slight changes do not appear to significantly alter the molecular structures of the cavities of Host **1** as compared to CB[7]. The basic packing of the individual Host **1•16** complexes can be seen in Figure II-2 (b-c).

a)

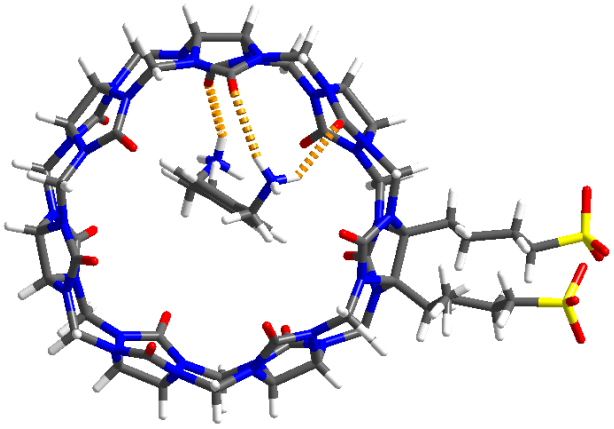

b)

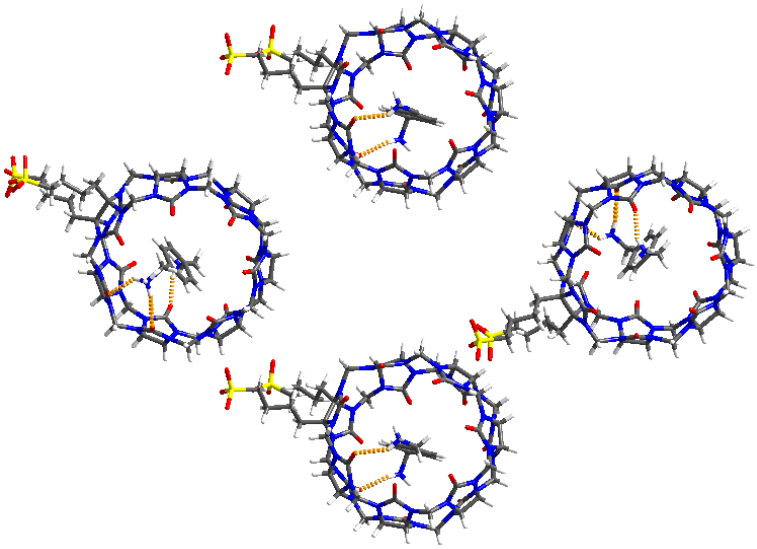

c)

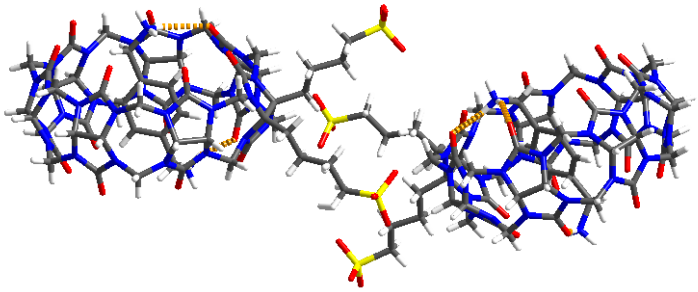

Figure II-2. (a) the crystal structure of Host **1•16** and (b) a portion of the crystal lattice showing the three-dimensional packing motif down the a-axis. (c) a portion of the crystal lattice showing the three-dimensional packing motif down the b-axis. Color code: C, grey; H white; N, blue; O, red; S, yellow; H-bonds, orange-striped.

2.2.4 Investigation of the Availability of the Cavity of Host 1 for Binding

^{1}H NMR spectroscopy was used to investigate the potential intermolecular self-association between the $(CH_2)_4SO_3Na$ arms and an adjacent cavity (Figure II-3). Dilution experiments were performed on Host **1** solutions ranging from 16 mM to 130 μM. The methylene signals of the $(CH_2)_4SO_3Na$ arms appear at 2.90, 2.40, 1.80, and 1.39 ppm, respectively, throughout the concentrations investigated. A lack of upfield shift at any concentration indicated the methylene protons are not encapsulated by another Host **1** compound. These encouraging results indicate the butyl arms are not able to associate with the cavity of an adjacent molecule of Host **1** and the cavity is therefore free to encapsulate a guest molecule.

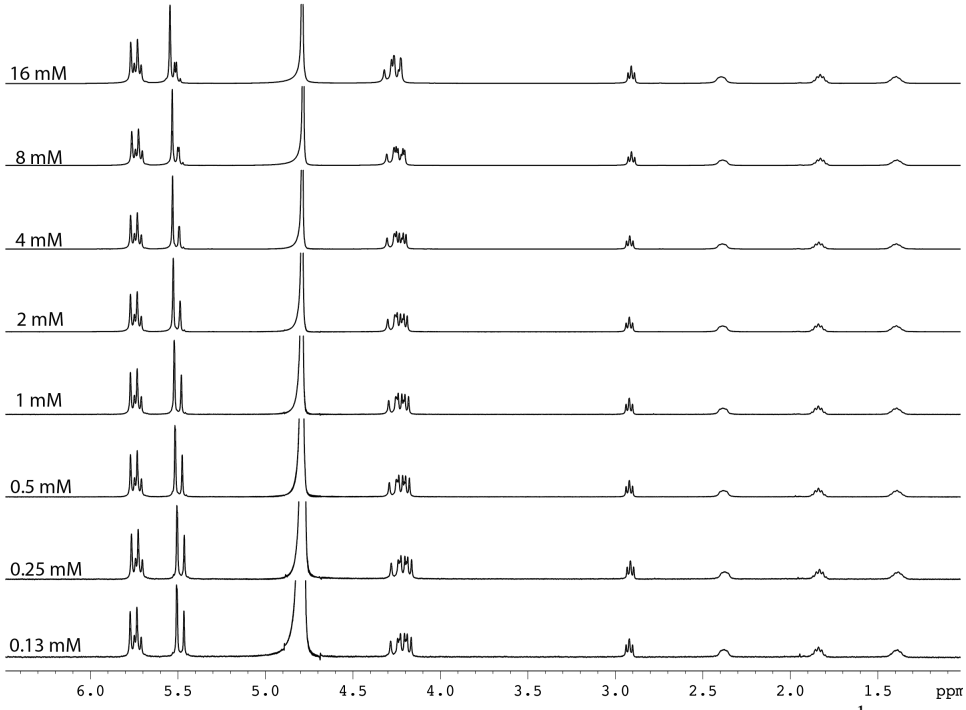

Figure II-3. Dilution experiments performed with Host **1** monitored by ^{1}H NMR (D_2O, 400 MHz, RT).

2.2.5 Molecular Recognition Properties of Host 1

Once it was confirmed that the cavity is available for guest complexation, the molecular recognition properties of Host **1** were qualitatively investigated. Typical CB[*n*] guests ranging from hexanediamine•2HCl (**13**) to 1-adamantyl amine•HCl (**14)** were selected for this purpose (Appendix). The binding study for **13** did not reveal any surprises. Figure II-4 (b) shows the typical upfield shift for the methylene protons inside the cavity. The appearance of sharp signals for both the free and bound guests of a 1:2 host:guest mixture indicates that the exchange is slow on the ^{1}H NMR chemical shift timescale (Figure II-4 (c)). All of the Host **1**•guest complexes studied show very similar guest resonances to their CB[7]•guest complex counterparts. This similarity indicated comparable magnetic environments of the two cavities as we presumed. These reassuring results confirm the recognition properties of Host **1** are similar to those of CB[7].

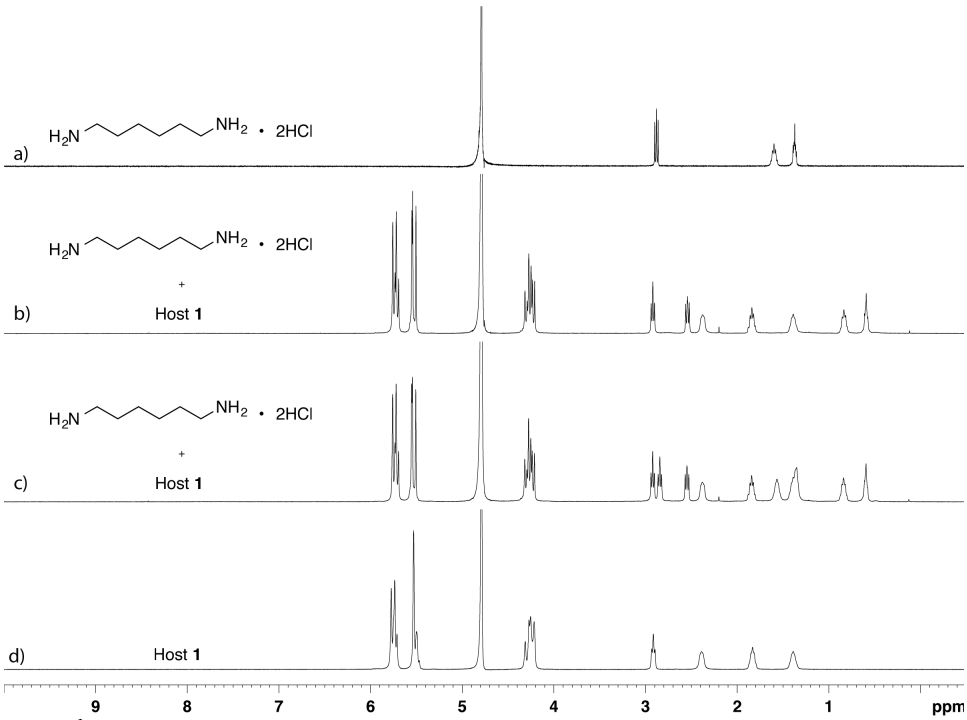

Figure II-4. ^{1}H NMR spectra (400 MHz, D_2O, room temperature) recorded for a mixture of (a) **13** (1 mM), (b) 1:1 mixture Host **1** (1 mM) and **13** (1 mM), (c) 1:2 mixture Host **1** (1 mM) and **13** (2 mM), (d) Host **1** (1 mM).

2.2.6 Drug Solubilization Using Host 1

Although the expected solubility enhancement of host **1** vs. CB[7] was not observed, the molecular recognitions properties of Host **1** appeared to be intact. Therefore we decided to investigate the use of Host **1** as an excipient for drug solubilization. Perhaps the sulfonate groups could enhance the aqueous solubility of the host•guest complex. To test this hypothesis, we constructed phase solubility diagrams.[29] To construct a phase solubility diagram, a solution of a known concentration of container was stirred with an excess of insoluble drug at room temperature in either a 50 mM sodium sodium acetate buffer at pD = 4.74 or a 10% DCl solution in D_2O until equilibrium was reached. The mixtures were then centrifuged and the pellet was discarded. The concentrations of the host and drug in the supernatant were determined by spiking the ^{1}H NMR samples with a known concentration of $MeSO_3H$ or benzene-1,3,5-tricarboxylate sodium salt as non-binding internal standards.

The phase solubility diagram of albendazole (**17**) was obtained in a 50 mM sodium acetate buffer at pD = 4.74 revealing the similar binding properties of Host **1** and CB[7] (Figure II-5). Eq. 1 assumes 1:1 host:guest binding which should have a linear slope where s_0 is the intrinsic solubility of the free guest. The graph is linear throughout the entire concentration range available at pD = 4.74 which is interpreted as 1:1 host:guest binding for Host **1** and CB[7] with **17** as expected. The similar slopes for Host **1** and CB[7] even indicate similar K_a's. However, the limited water solubility of the hosts do not allow for further investigation of the binding properties past the linear region. We must conclude that the addition of the sulfonate arms on Host **1** are able to enhance the

solubility of **17** to a greater extent than Me_2CB[7], but unfortunately are unable to enhance the water solubility of the Host **1•17** complex past that of CB[7]•**17**.

$$K_a = \frac{slope}{s_0(1-slope)} \quad (1)$$

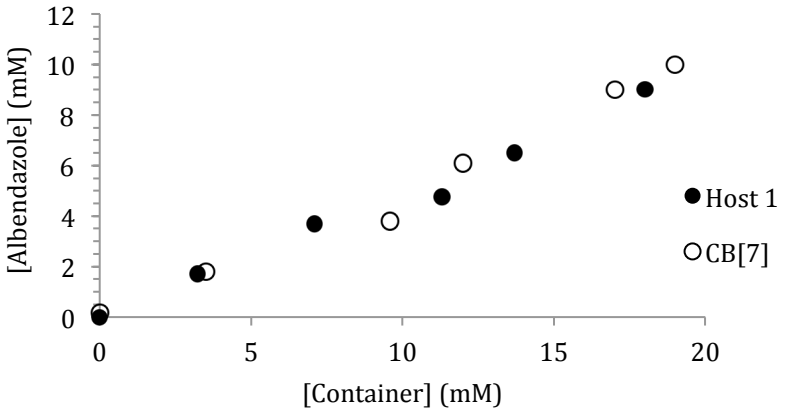

Figure II-5. Phase solubility diagram for **17** with CB[7] and Host **1**.

Camptothecin (**18**) is present in two forms in aqueous solutions, the concentrations of which are pH dependent. In solutions of pH > 7.2 the carboxylate is the prevalent form while in solutions of pH < 4 the lactone is most prevalent and able to associate with a CB[*n*] host. We wanted to investigate the ability of Host **1** to act as an excipient for **18** at a pH slightly greater than 4. Regrettably, the lactone concentration was too low in a sodium acetate buffer at pH = 4.74; therefore the phase solubility diagram of **18** was obtained using a 0.01 M DCl solution in D_2O at pD = 2 (Figure II-6). Similar association of **18** between Host **1** and CB[7] was also indicated by the linear phase solubility diagrams and 1:1 host:guest binding was inferred. The low water solubility of the hosts do not allow for further investigation of the binding properties past the linear region. Disappointingly, the sulfonate arms are not able to enhance the water solubility of the Host **1•18** complex compared to CB[7]•**18**.

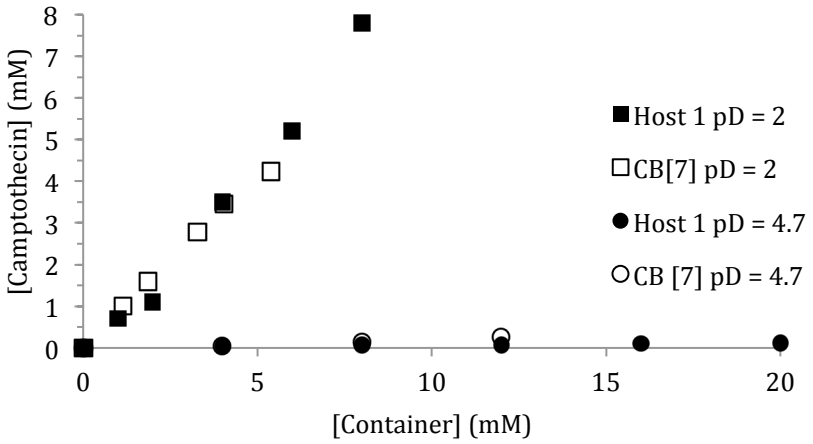

Figure II-6. Phase solubility diagram for **18** with CB[7] and Host **1**.

Interestingly, the phase solubility diagram for the antihistamine cinnarizine (**12**) in a 50 mM sodium acetate buffer at pD = 4.74 shows a significant difference between Host **1** and CB[7] complexation (Figure II-7). The phase solubility diagram for CB[7] is linear, indicating the expected 1:1 host:guest binding. However, the phase solubility diagram for Host **1** indicates a highly reduced solubility for the Host **1•12** complex. This is a surprising result since all previously gathered evidence indicates comparable binding properties between the similar cavities of Host **1** and CB[7]. Further data was not gathered to determine the cause of this change in solubility.

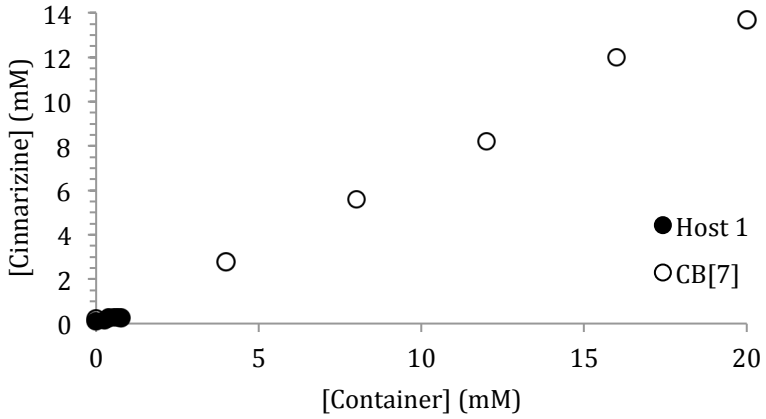

Figure II-7. Phase solubility diagram for **12** with CB[7] and Host **1**.

2.4 Conclusion

In summary, a new difunctionalized cucurbit[7]uril (Host **1**) was synthesized using the unique building-block approach by the condensation reaction between functionalized glycoluril bis(cyclic ether) (**30**) and glycoluril hexamer (**21**) in moderate yield (28%). Contrary to our hypothesis, the addition of two $(CH_2)_4SO_3Na$ arms did not enhance the aqueous solubility of Host **1** relative to CB[7]. The similar molecular recognition properties of Host **1**, as compared to CB[7], led us to investigate the possibility of Host **1** to be a suitable excipient for drug delivery. Unfortunately, the drug solubility enhancement studies showed that the addition of the $(CH_2)_4SO_3Na$ arms did not, in fact, enhance the solubility of the Host **1**:drug complex as desired.

Appendix

Synthesis and Recognition Properties of a CB[7] Derivative Bearing Sulfonate Functional Groups

Supporting Information

*By Lorene E. Brownlow, Peter Y. Zavalij, and Lyle Isaacs**

Department of Chemistry and Biochemistry, University of Maryland, College Park, MD 20742

Table of Contents **Pages**

General Experimental. Starting materials were purchased from commercial suppliers and were used without further purification. N,N'-diisopropyl-1,2-butanediimine (**24**) and glycoluril hexamer (**21**) were prepared according to literature procedures.[1-2] Melting points were measured on a Meltemp apparatus in open capillary tubes and are uncorrected. IR spectra were recorded on a JASCO FT/IR 4100 spectrometer and are reported in cm^{-1}. NMR spectra were measured on spectrometers operating at 400 or 500 MHz for ^{1}H and 100 or 125 MHz for ^{13}C NMR spectra and are reported in ppm. Mass spectrometry was performed using a JEOL AccuTOF electrospray instrument (ESI).

Synthetic Procedures and Characterization.

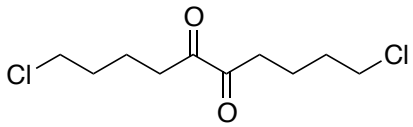

Compound 27. A solution of LDA in THF/heptane/ethylbenzene (2.0 M, 137 mL, 274 mmol) was added slowly over 90 min. to a stirring solution of N,N'-diisopropyl-1,2-butanediimine (20.0 g, 119 mmol) in distilled THF (180 mL) under N_2, maintained at -78 ˚C and stirred for an additional 5 h. A solution of 1-chloro-3-iodopropane (57.4 g, 280 mmol) in distilled THF (20 mL) was added over 15 min. and the mixture was stirred at -78 ˚C under N_2. After 15 h, aqueous HCl (1 M, 600 mL) was added and the mixture was allowed to stir at RT for 5 h. THF was removed under reduced pressure, and CH_2Cl_2 (160 mL × 3) was used to extract the product from the remaining aqueous layer. The organic layers were combined and washed with HCl (1 M, 60 mL), H_2O (120 mL), and sat. $NaHCO_3$ (120 mL), and the organic layer was then dried over $MgSO_4$. The mixture was filtered and the filtrate was concentrated under reduced pressure to yield a crude orange oil. The oil was purified by distillation (133-137 ˚C/0.08 mm Hg) to give the product

(22.5 g, 94.1 mmol, 79%) as a yellow oil. ^{1}H NMR (500 MHz, $CDCl_3$): 3.55 (t, J = 6.3, 4H), 2.79 (t, J = 7.1, 4H), 1.85-1.70 (m, 8H). ^{13}C NMR (125 MHz, $CDCl_3$): 198.9, 44.4, 35.1, 31.7, 20.2. ESI-MS: *m/z* 241 ($[M + H]^+$, calcd. for $C_{10}H_{17}{}^{35}Cl^{37}ClO_2^+$, 241.1755).

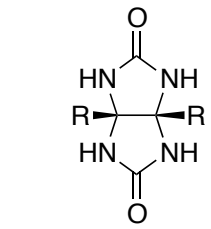

R = $CH_2CH_2CH_2CH_2Cl$

Compound 28. Benzene (70 mL) was added to a round bottom flask that was equipped with a Dean-Stark apparatus and heated to reflux while stirring under N_2. After 1 h, **27** (8.00 g, 33.5 mmol), urea (10.0 g, 167 mmol), and TFA (3.00 mL, 39.2 mmol) were added to the round bottom flask. The mixture was refluxed while stirring under N_2 with the Dean-Stark apparatus for 4 h, and then allowed to cool to RT. EtOH (200 mL) was added to the round bottom flask, which caused a precipitate to form. The white solid was collected by filtration and washed with EtOH (100 mL × 3), and dried under high vacuum for 16 h to yield the product as a white powder (3.21 g, 9.94 mmol, 30%). M.p. 220-222 ˚C. IR (ATR, cm^{-1}): 3206m, 2955w, 1669s, 1497m, 1459m, 1306w, 1174m, 1108m, 1063m, 1007w. ^{1}H NMR (400 MHz, DMSO-d_6): 7.16 (s, 4H), 3.63 (t, J = 6.7, 4H), 1.73 (q, J = 6.7, 4H) 1.70-1.45 (m, 8H). ^{13}C NMR (100 MHz, DMSO-d_6): 159.8, 77.6, 45.1, 34.0, 32.4, 20.1. ESI-MS: *m/*z 323 ($[M + H]^+$). HR-MS: *m/z* 323.1056 ($[M + H]^+$, calcd. for $C_{12}H_{21}{}^{35}Cl_2N_4O_2^+$, 323.1042).

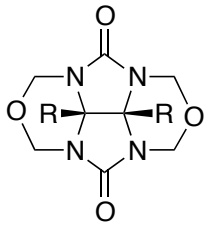

R = $CH_2CH_2CH_2CH_2Cl$

Compound 29. Compound **28** (8.80 g, 27.2 mmol), formalin (37% aqueous solution, 11.0 mL, 147 mmol), and HCl (9 M, 26.0 mL) were added to a round bottom flask which was capped

with a polyethylene stopper. The mixture was allowed to stir at RT for 20 h and then H_2O (150 mL) was added. After an additional day of stirring, the precipitate was collected by filtration, washed with H_2O (100 mL × 3) and dried under high vacuum for 16 h to yield the product as a gray solid (10.4 g, 25.8 mmol, 94%). M.p. 134-137 ˚C. IR (ATR, cm^{-1}): 2950w, 1718s, 1419s, 1236m, 1173s, 1011s, 891s, 722s. ^1H NMR (400 MHz, $CDCl_3$): 5.52 (d, *J* = 11.4, 4H), 4.75 (d, *J* = 11.4, 4H), 3.60 (t, *J* = 6.2, 4H), 2.30-2.20 (m, 4H), 1.95-1.85 (m, 4H), 1.65-1.50 (m, 4H). ^{13}C NMR (100 MHz, $CDCl_3$): 158.1, 75.7, 71.3, 44.4, 32.1, 28.7, 21.6. ESI-MS: *m/z* 407 ($[M + H]^+$). HR-MS: *m/z* 407.1233 ($[M + H]^+$, calcd. for $C_{16}H_{25}{}^{35}Cl_2N_4O_4^+$, 407.1253).

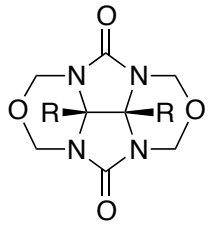

R= $CH_2CH_2CH_2CH_2SO_3Na$

Compound 30. **29** (3.00 g, 7.37 mmol) and Na_2SO_3 (4.60 g, 36.8 mmol) were mixed in a round bottom flask. H_2O (60.0 mL) was added and the mixture was refluxed while stirring for 72 h. After cooling to RT the solvent was removed under reduced pressure and the solid was stirred in MeOH (100 mL × 3) for 24 h. The mixture was filtered and reduced pressure was used to remove MeOH from the combined filtrates to yield the product as a white solid (2.00 g, 3.68 mmol, 50%). M.p. >300˚C. IR (ATR, cm^{-1}): 2933w, 1743m, 1419m, 1171s, 1034s, 983m, 916m, 735m. ^1H NMR (500 MHz, D_2O): 5.41 (d, *J* = 10.9, 4H), 5.06 (d, *J* = 10.9, 4H), 2.96 (t, *J* = 7.1, 4H), 2.42 (t, *J* = 8.0 4H), 1.87 (q, *J* = 7.4, 4H), 1.55 (q, *J* = 7.4, 4H). ^{13}C NMR (125 MHz, D_2O, 1,4-dioxane as internal reference): 159.0, 76.2, 70.4, 49.9, 27.1, 23.5, 21.6. ESI-MS: *m/z* 248 ($[M - 2Na]^{2-}$). HR-MS: *m/z* 248.0453 ($[M - 2Na]^{2-}$, calcd. for $C_{16}H_{24}N_4O_{10}S_2{}^{2-}$, 248.0467).

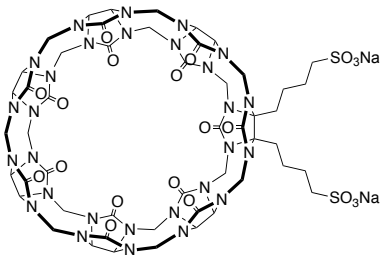

((CH$_2$)$_4$SO$_3^-$)$_2$ CB[7] Host **1-3**. Compound **21** (1.50 g, 1.54 mmol), KCl (0.229 g, 3.09 mmol), and conc. HCl (7.5 mL) were added to a round bottom flask. The mixture was stirred at RT for approximately 1 min. until all components dissolved, at which time **30** (1.68 g, 3.09 mmol) was added. The flask was then sealed with a rubber septum and stirred at 100 °C for 30 min. The reaction mixture was then poured into a 50 mL centrifuge tube containing MeOH (40 mL), which resulted in a red-brown precipitate. The mixture was centrifuged at 7700 rpm for 7 min. The supernatant was decanted, and an additional portion of MeOH (40 mL) was added, followed by sonication for 10 min. and centrifuged at 7700 rpm for 7 min. This process was repeated with two additional portions of MeOH (40 mL). The precipitate was dried under high vacuum to give a crude red-brown powder (2.34 g). ^{1}H NMR spectroscopy with **16** was used to determine the purity by integration of the Host **1•16** Ar-H hydrogens of **16** at 6.60 (s, 4H) versus that of the methylene/methine C-H hydrogens of Host **1** at 5.35-5.80 (m, 26H). This procedure allowed us to calculate that Host **1** comprised 46% of the crude solid. The crude solid was dissolved in H_2O (5 mL). This solution was loaded onto a column (3 cm diameter × 50 cm long) containing 35 cm Dowex 50WX2 ion-exchange resin pretreated with H_2O. The column was eluted with H_2O (600 mL). The fractional purity was assessed by ^{1}H NMR in the presence of **16**, using the same procedure above, and the appropriate fractions were combined. The solvent was removed under reduced pressure. H_2O (10 mL) was used to dissolve the solid, which was then precipitated in MeOH (40 mL). The solid was collected by centrifugation and suspended in H_2O (5.0 mL). The solution was adjusted to pH = 7.0 using a hydroxide solution (0.5 M aq.)

(NaOH for Host **1**, KOH for Host **2**, NH_4OH for Host **3**). The solvent was removed under reduced pressure and then dried further under high vacuum for 16 h to yield the product as a white solid (0.634 g, 0.429 mmol, 28%). Host **1** was fully characterized. M.p. >300 ˚C. IR (ATR, cm^{-1}): 1728m, 1465m, 1322m, 1231m, 1188m, 1035m, 963m, 802s, 759m, 671m. ^1H NMR (400 MHz, D_2O, >2 equiv. **16**, RT): 7.46 (s, unbound **16**), 6.60 (s, bound **16**, 4H), 5.77 (d, *J* = 15.1, 2H), 5.73 (d, *J* = 15.1, 4H), 5.70 (d, *J* = 15.3, 4H), 5.64 (d, *J* = 15.3, 4H), 5.57 (d, *J* = 8.6, 2H), 5.53 (d, *J* = 8.6, 2H), 5.50-5.35 (m, 8H), 4.29 (d, *J* = 15.6, 6H), 4.21 (d, *J* = 15.6, 4H), 4.13 (d, *J* = 15.6 4H), 3.91 (s, 4H), 2.92 (t, *J* = 7.2, 4H), 2.50-2.30 (m, 4H), 1.90-1.75 (m, 4H), 1.50-1.30 (m, 4H). ^{13}C NMR (125 MHz, D_2O, 1,4-dioxane as internal reference, >1 equiv **16**, RT): 156.2, 156.1, 155.9, 155.9, 133.0, 128.9, 127.3, 79.8, 71.3, 71.0, 70.9, 70.8, 70.6, 70.4, 52.6, 52.0, 51.7, 49.7, 48.7, 42.2, 42.1, 41.9, 41.8, 26.7, 23.4, 20.3, 19.2. ESI-MS: *m/z* 786 ($[M•\mathbf{16} - 2Na + 4H]^{2+}$). HR-MS: *m/z* 786.2488 ($[M - 2Na + PXDA + 4H]^{2+}$, calcd. for $[C_{58}H_{72}N_{30}O_{20}S_2]^{2+}$, 786.2490). The ^1H NMR spectra for Hosts **2** and **3** in the presence of **16** were congruent with that of Host **1**.

References:

1. N. D. Kimpe, L. D'Hondt, E. Stanoeva, *Tetrahedron Lett.* **1991**, *32*, 3879-3882.
2. L. Cao, G. Hettiarachchi, V. Briken, L. Isaacs, *Angew. Chem. Int. Ed.* **2013**, *52*, 12033-12037.

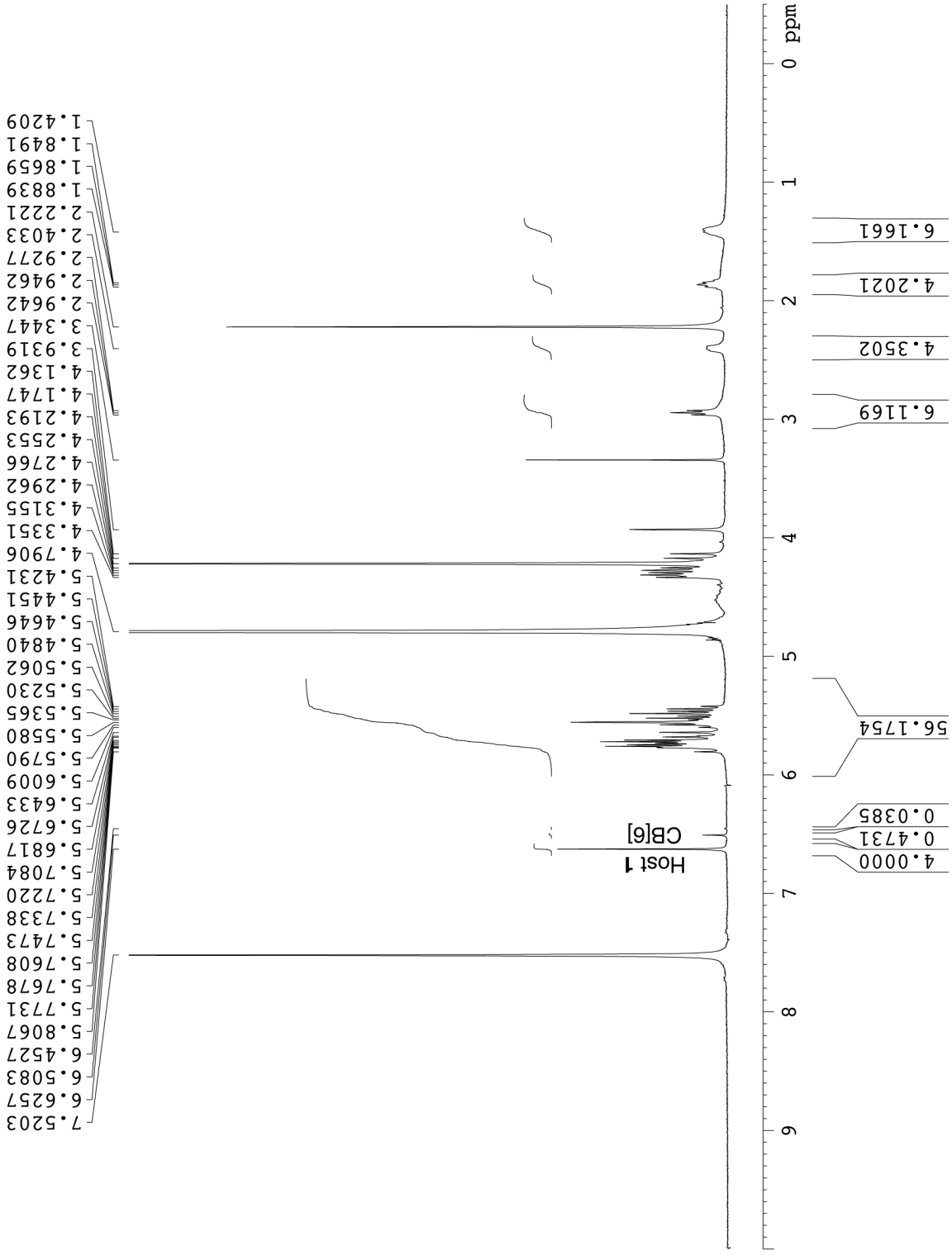

Figure S-1. ^{1}H NMR spectrum recorded (400 MHz, D_2O, RT) for the crude reaction mixture from the reaction between **21** and **30** in the presence of **16** as a probe. ^{1}H NMR integration of the **16** binding region (6-7 ppm) versus the methylene/methine region of Host **1** (5.4-5.8 ppm) allows us to determine the contents of the crude mixture (46% Host **1**, 5 % CB[6], 49% unidentified).

Figure S2. ^{1}H NMR spectrum recorded (500 MHz, $CDCl_3$, RT) for compound **27**.

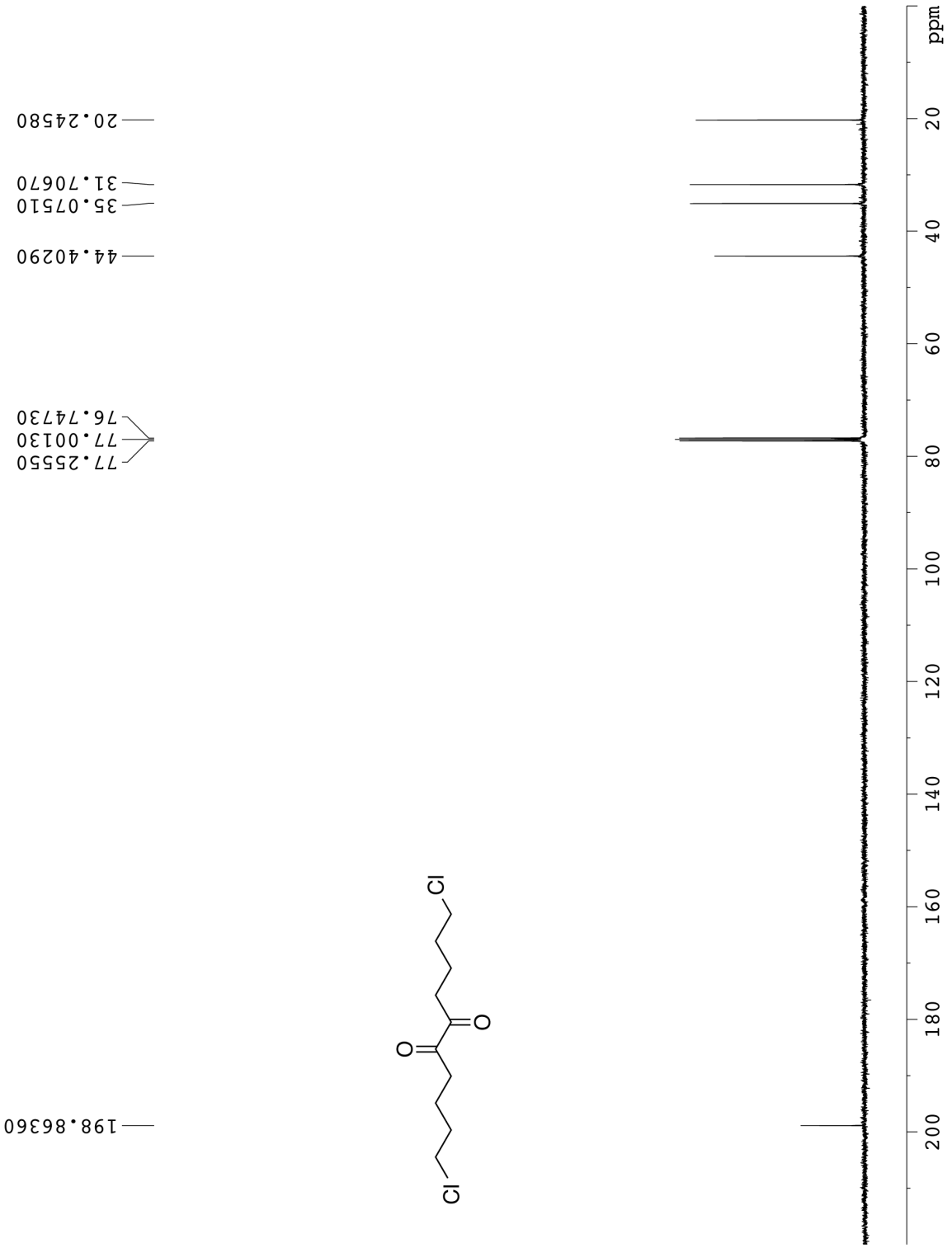

Figure S3. ^{13}C NMR spectrum recorded (125 MHz, $CDCl_3$, RT) for compound **27**.

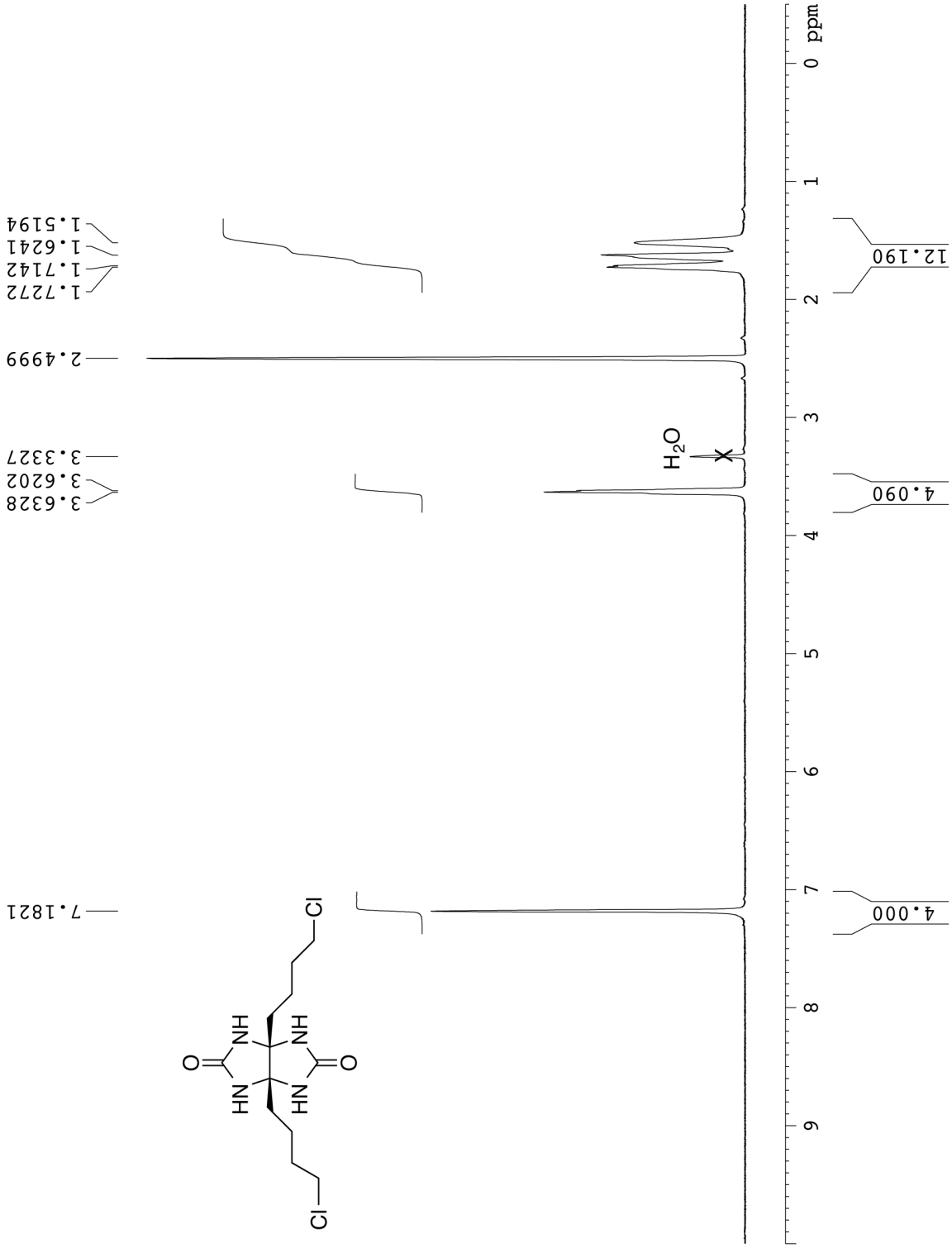

Figure S4. ^{1}H NMR spectrum recorded (400 MHz, DMSO-d_6, RT) for compound **28**.

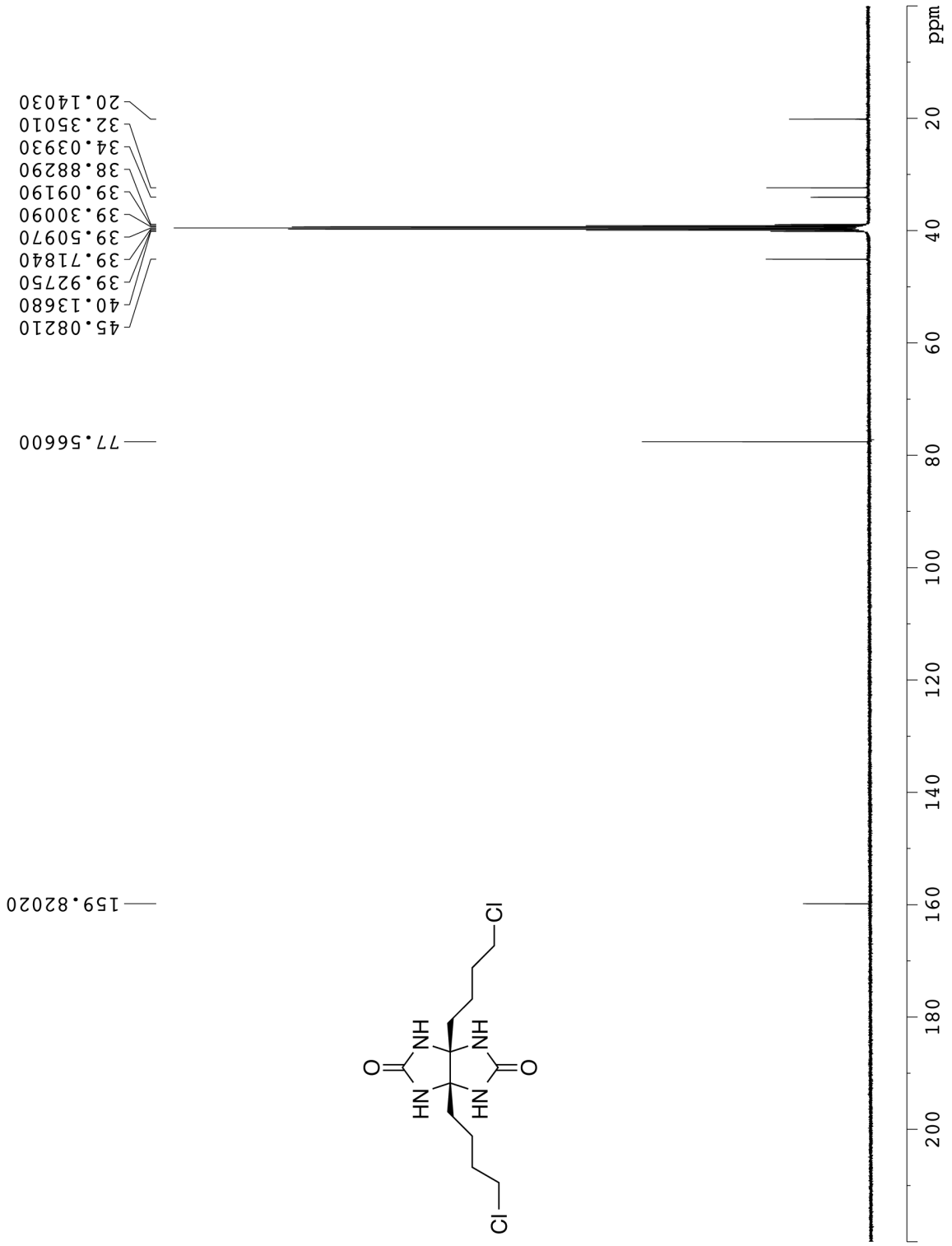

Figure S5. ^{13}C NMR spectrum recorded (100 MHz, DMSO-d_6, RT) for compound **28**.

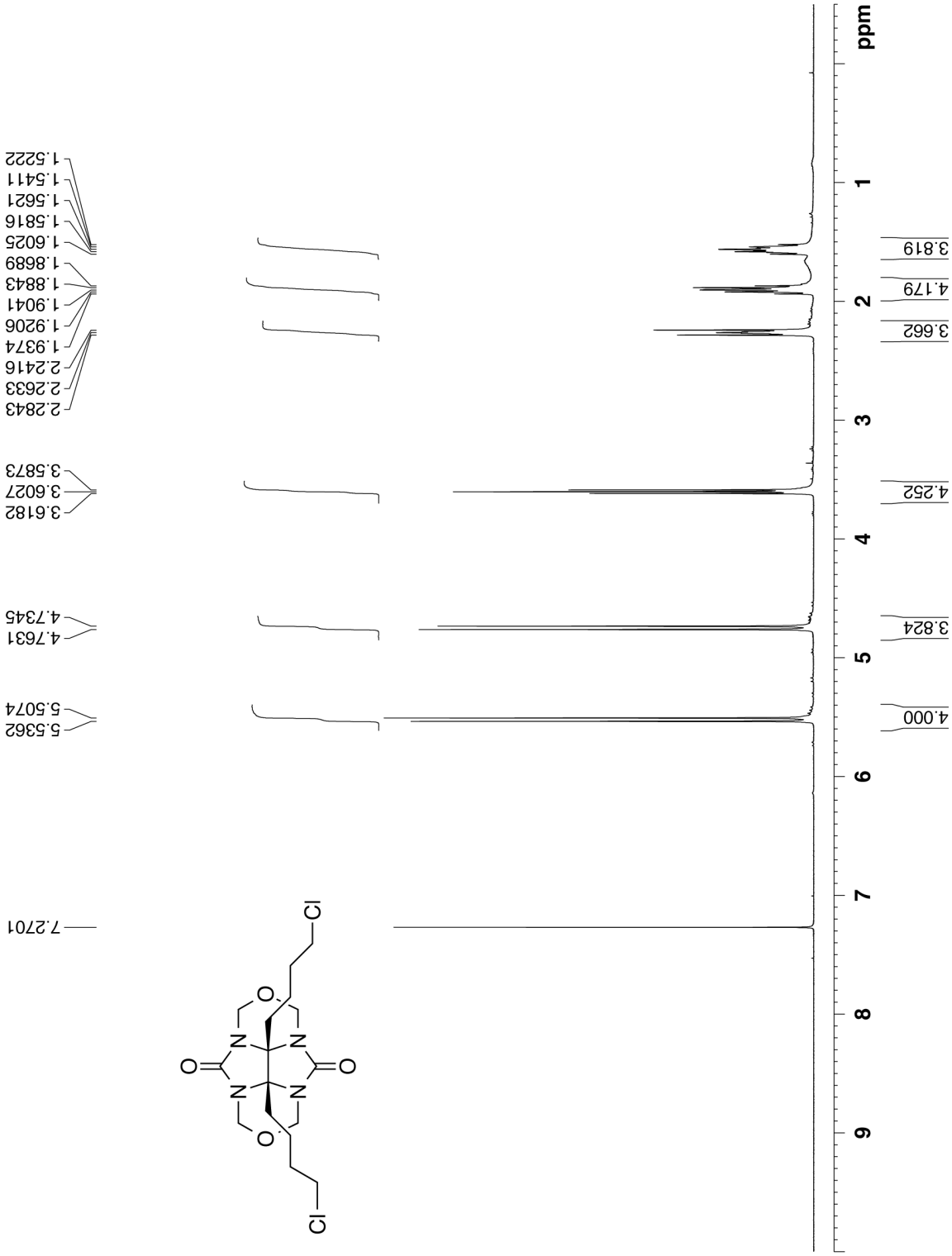

Figure S6. ^{1}H NMR spectrum recorded (400 MHz, $CDCl_3$, RT) for compound **29**.

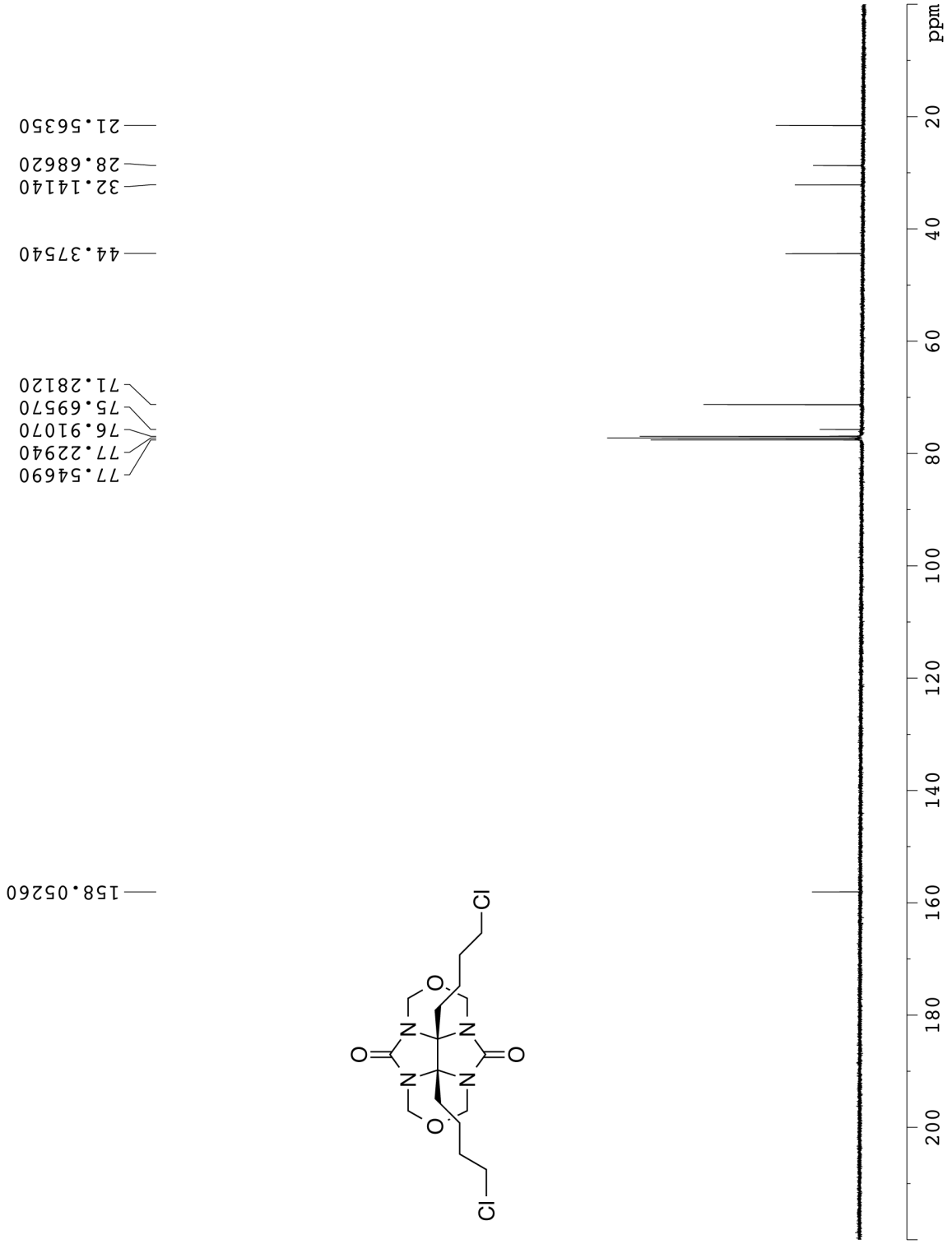

Figure S7. ^{13}C NMR spectrum recorded (100 MHz, $CDCl_3$, RT) f for compound **29**.

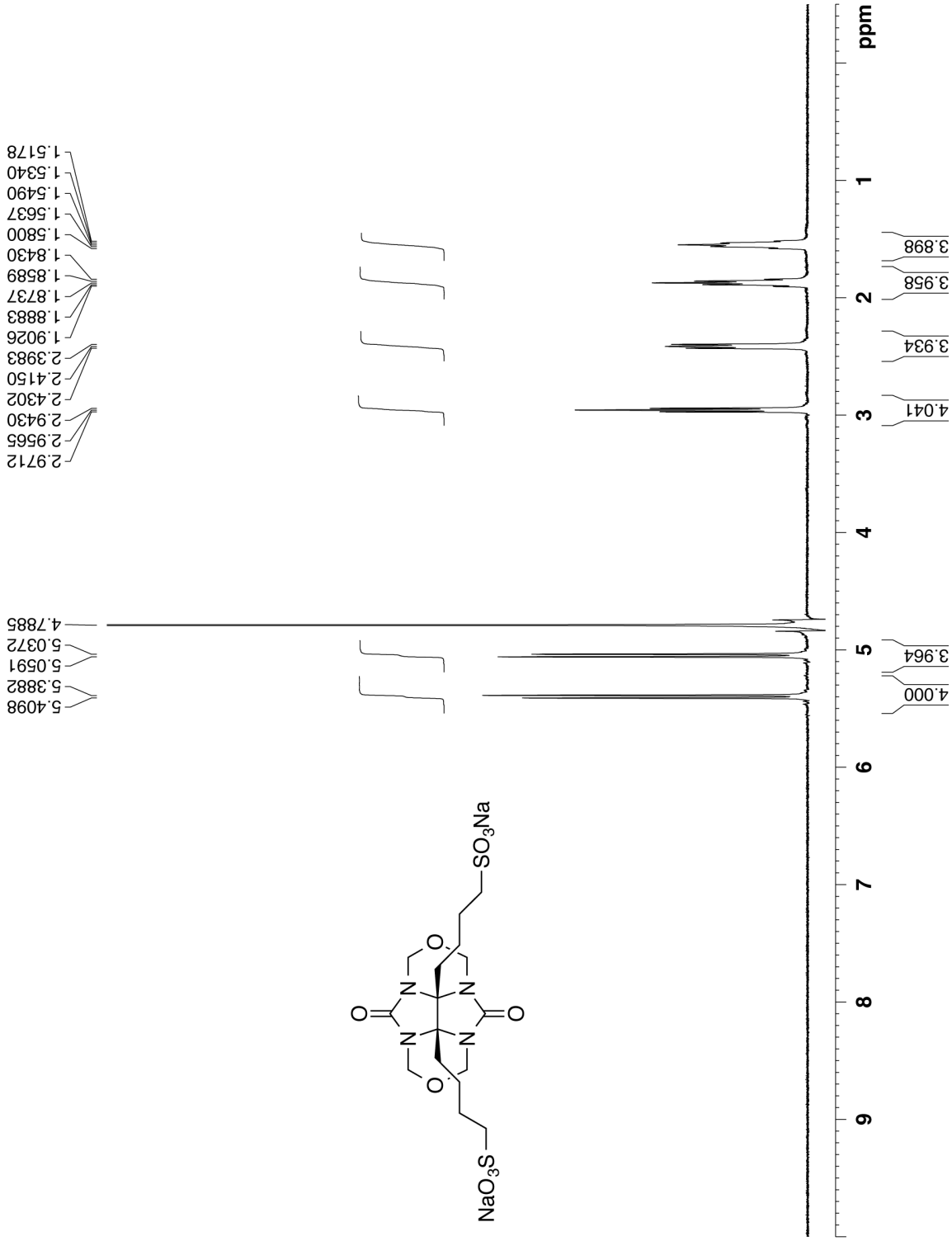

Figure S8. ^{1}H NMR spectrum recorded (500 MHz, D_2O, RT) for compound **30**.

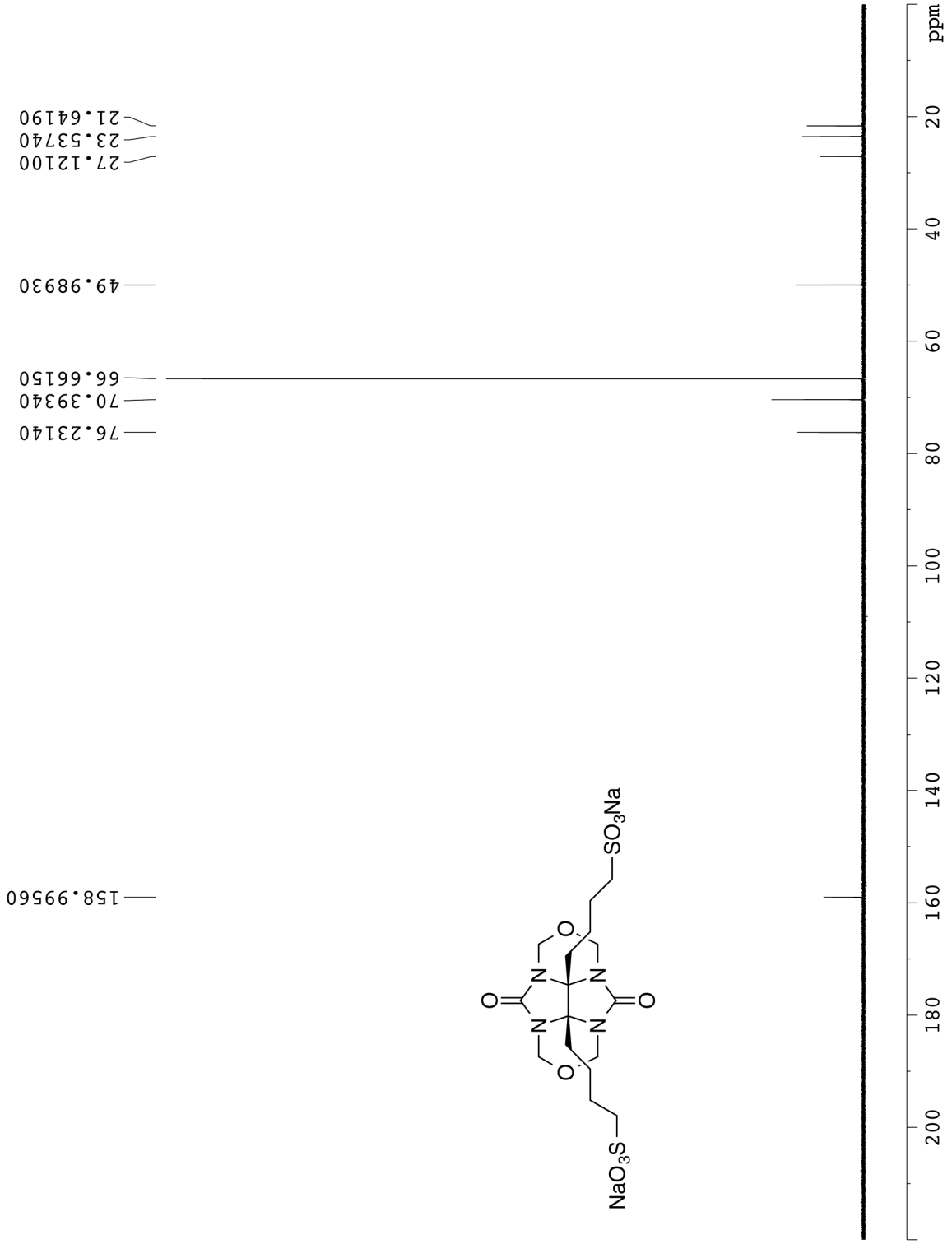

Figure S9. ^{13}C NMR spectrum recorded (125 MHz, D_2O, 1,4-dioxane as internal reference, RT) for compound **30**.

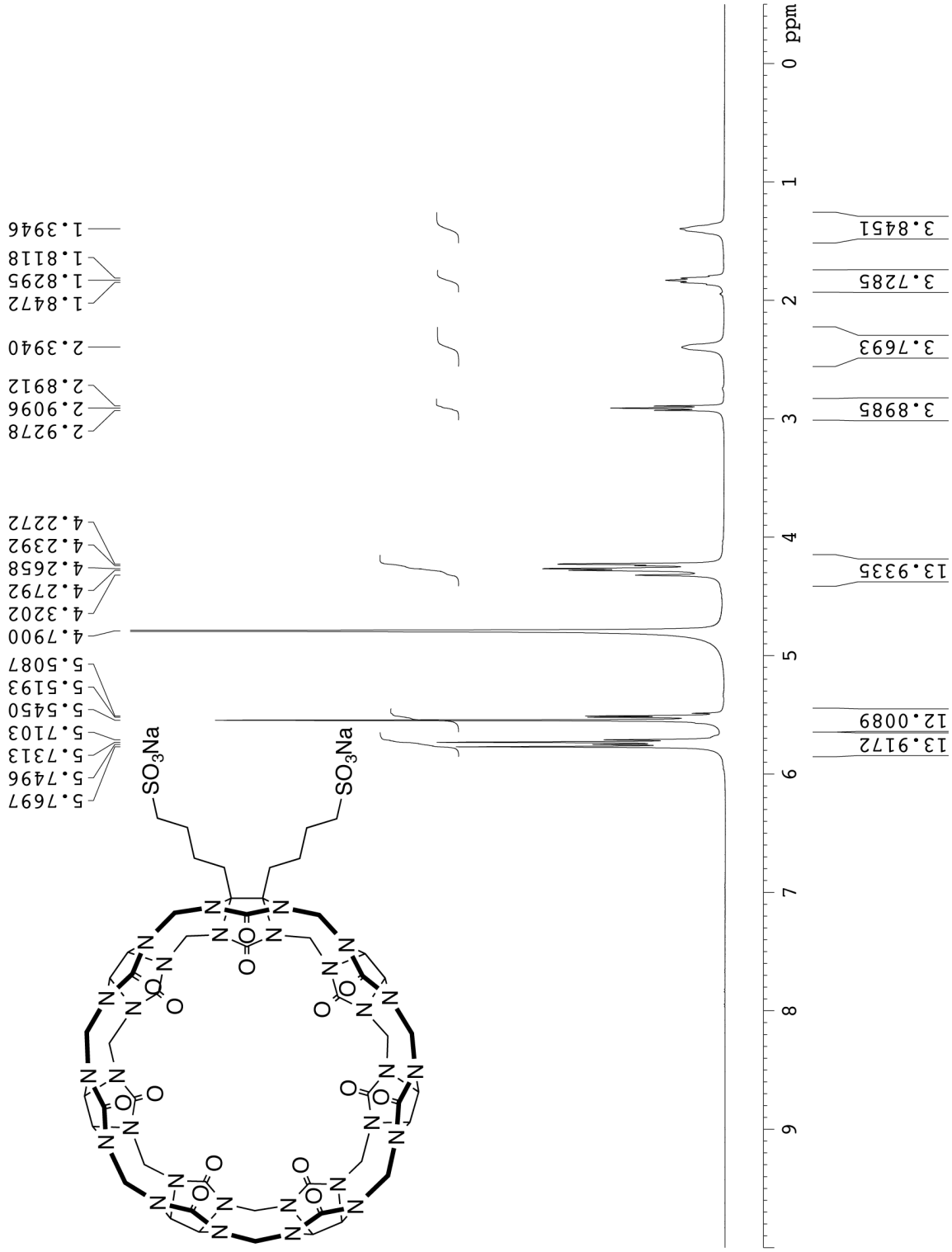

Figure S10. ^{1}H NMR spectrum recorded (400 MHz, D_2O, RT) for Host **1**.

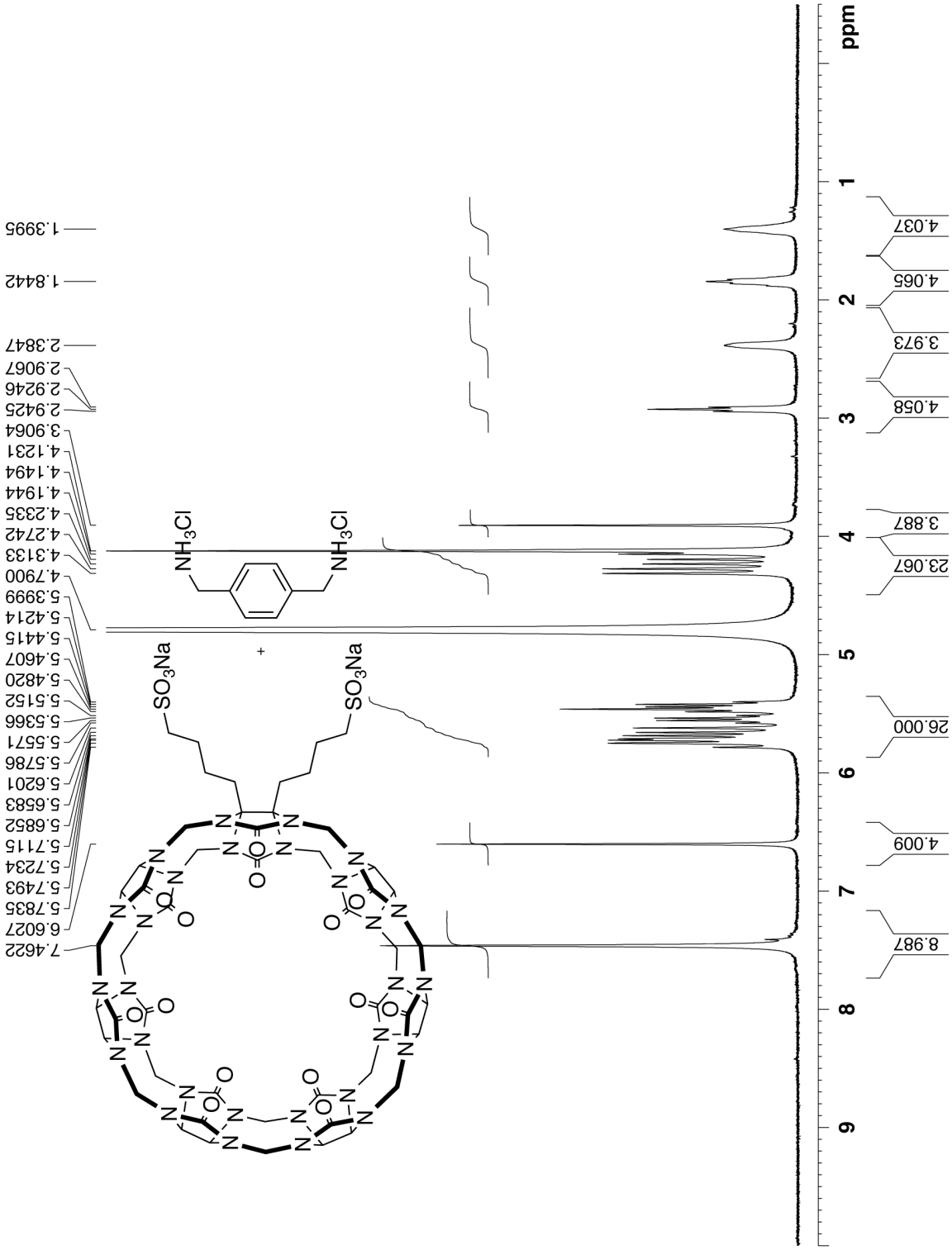

Figure S11. ^{1}H NMR spectrum recorded (400 MHz, D_2O, >2 equiv. **16**, RT) for Host **1**.

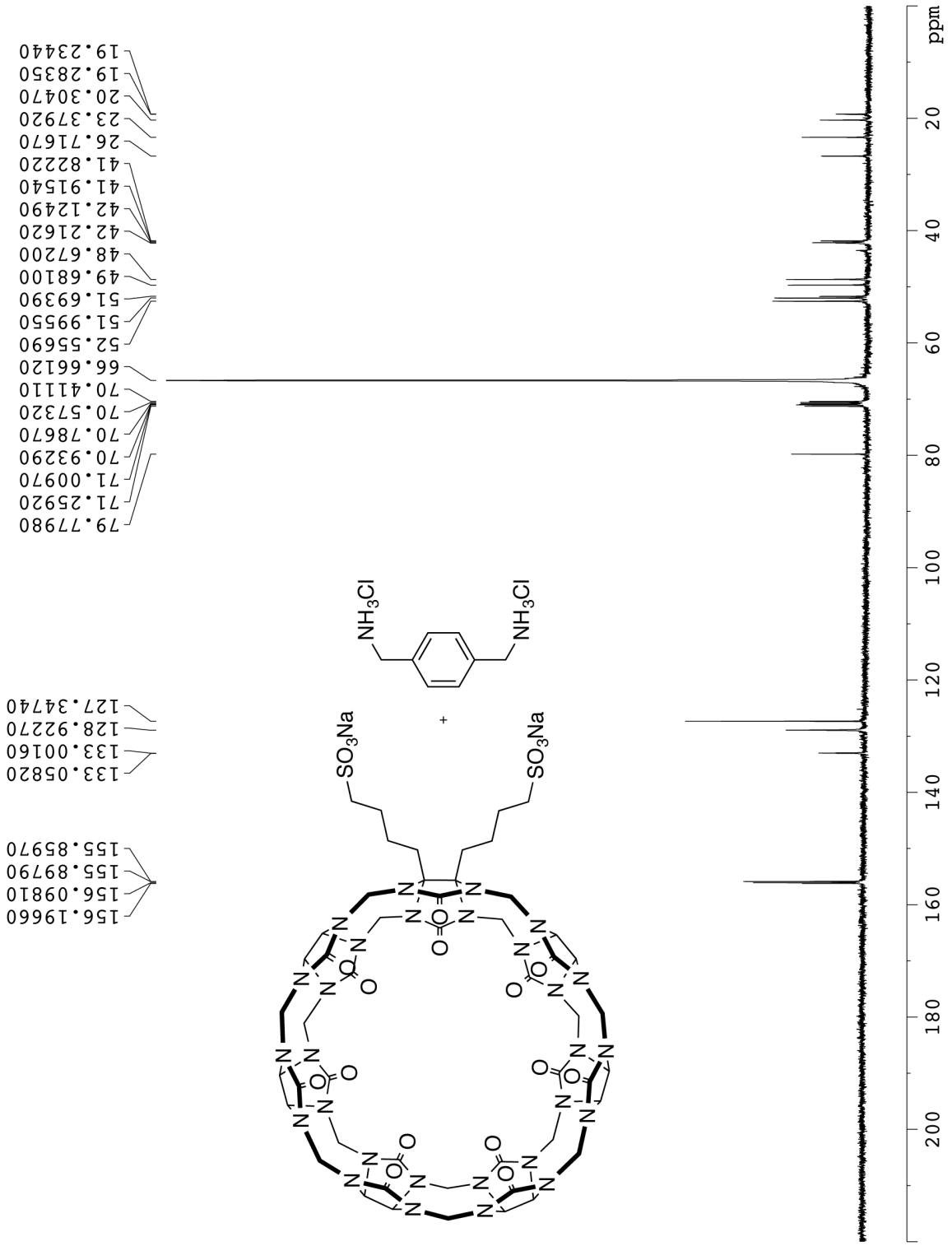

Figure S12. ^{13}C NMR spectrum recorded (125 MHz, D_2O, 1,4-dioxane as internal reference, >1 equiv. **16**, RT) for Host **1**.

Procedure to test the solubility of Hosts 1-3 in water. An excess of the host compound was added into 1 mL D_2O and magnetically stirred at room temperature for 16 h. The mixture was then centrifuged for two 10 min segments at 4400 rpm. A portion of the supernatant (420 μL) was combined with $MeSO_3H$ (200 mM, 40 μL in D_2O). The concentration of **1** was determined by the comparison of ^1H NMR resonance integrations of $MeSO_3H$ (2.78 ppm) versus the methylene/methine H-atoms of Host **1** (5.52-5.77 ppm) (Figure S13).

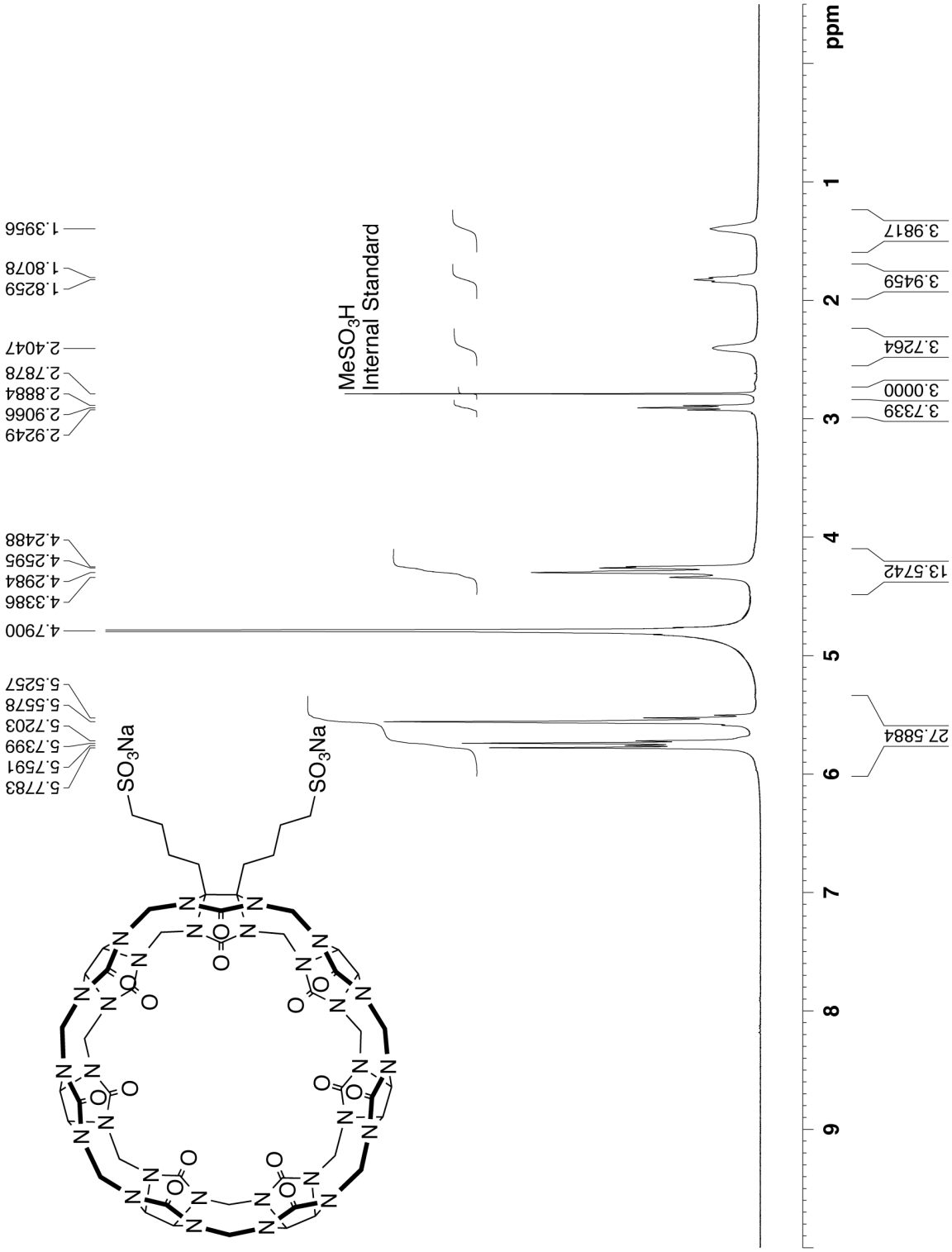

Figure S13. ^{1}H NMR spectra recorded (D_2O, 400 MHz, RT, 200 mM $MeSO_3H$ as internal reference) for Host **1**. The solubility of Host **1** is calculated to be 20.2mM.

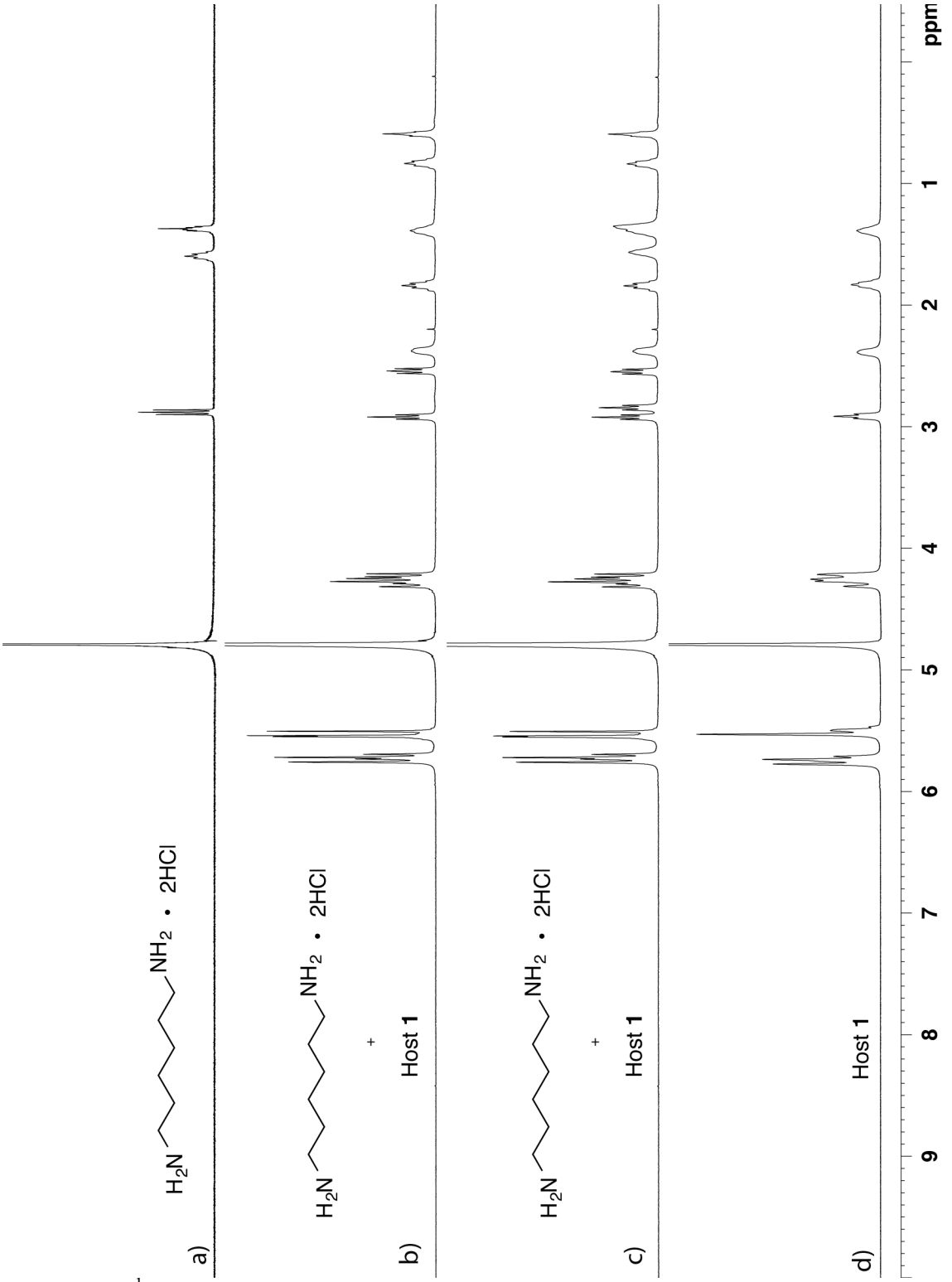

Figure S14. ^{1}H NMR spectra recorded (D_2O, 400 MHz, RT) for a) **13** (1 mM), b) a 1:1 mixture of Host **1** (1 mM) and **13** (1 mM), c) a 1:2 mixture of Host **1** (1 mM) and **13** (2 mM), d) Host **1** (1 mM).

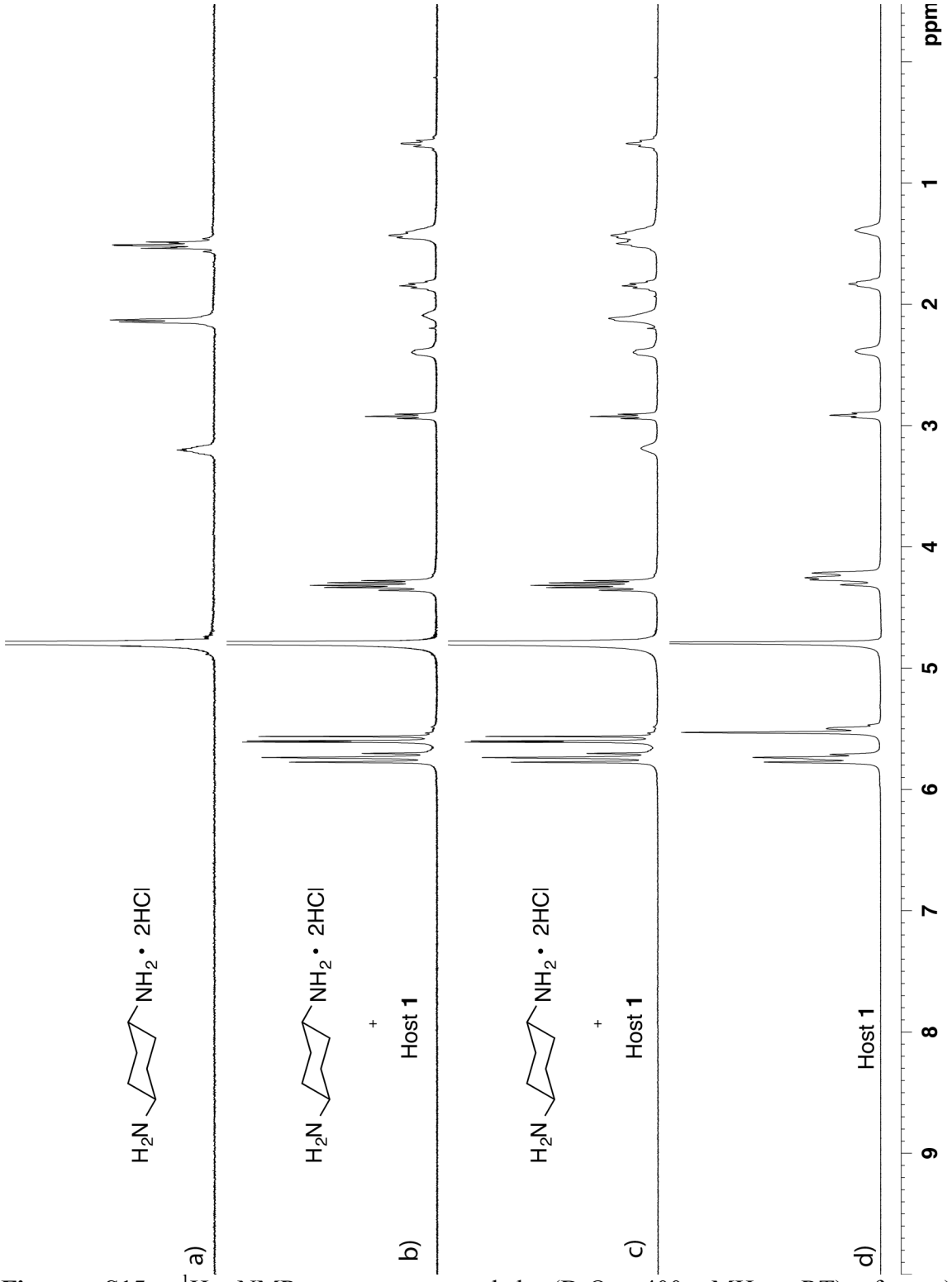

Figure S15. ^1H NMR spectra recorded (D_2O, 400 MHz, RT) for a) cyclohexanediamine•2HCl (1 mM), b) a 1:1 mixture of Host **1** (1 mM) and cyclohexanediamine•2HCl (1 mM), c) a 1:2 mixture of Host **1** (1 mM) and cyclohexanediamine•2HCl (2 mM), d) Host **1** (1 mM).

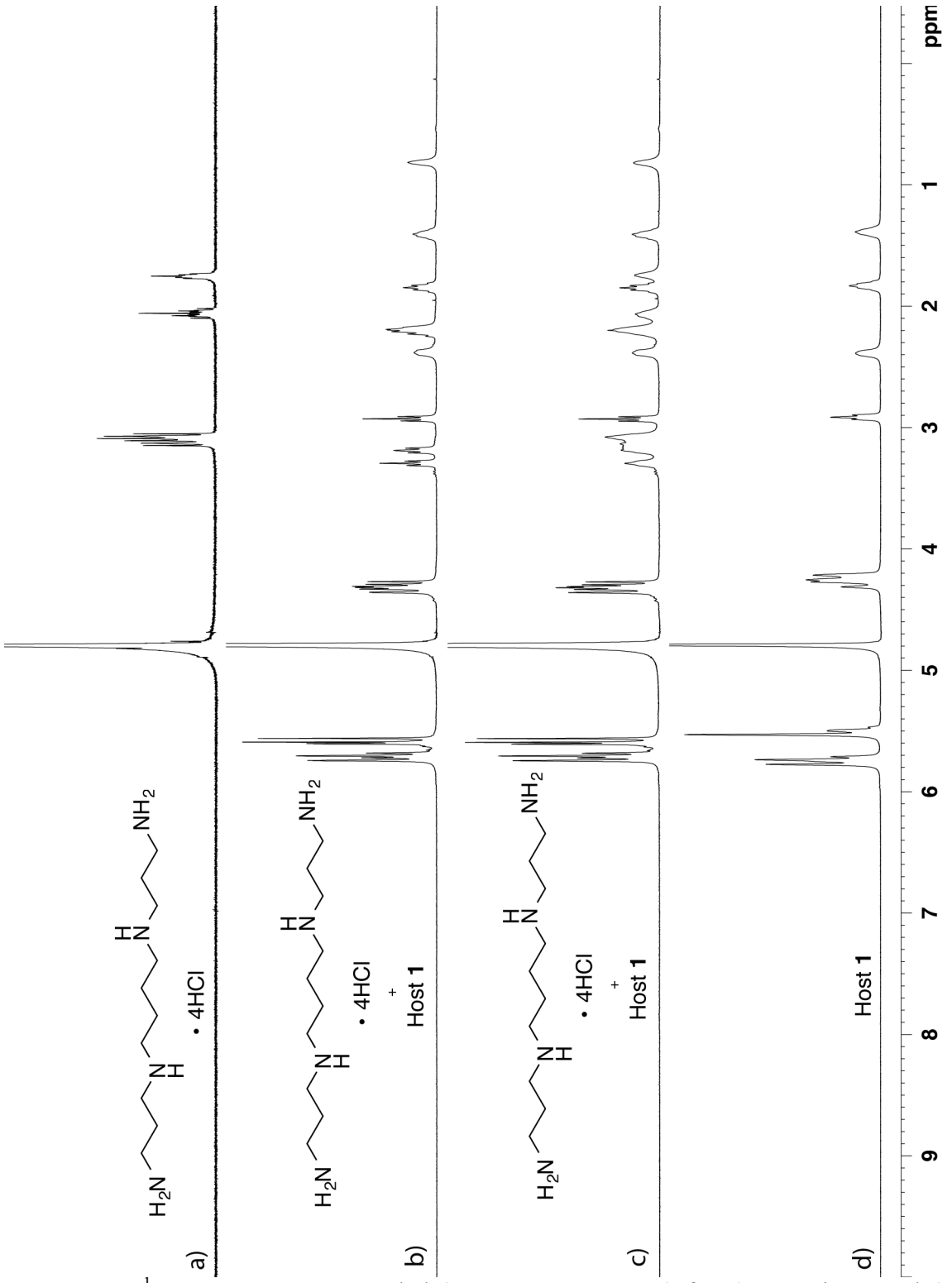

Figure S16. ^{1}H NMR spectra recorded (D_2O, 400 MHz, RT) for a) spermine•4HCl (1 mM), b) a 1:1 mixture of Host **1** (1 mM) and spermine•4HCl (1 mM), c) a 1:2 mixture of Host **1** (1 mM) and spermine•4HCl (2 mM), d) Host **1** (1 mM).

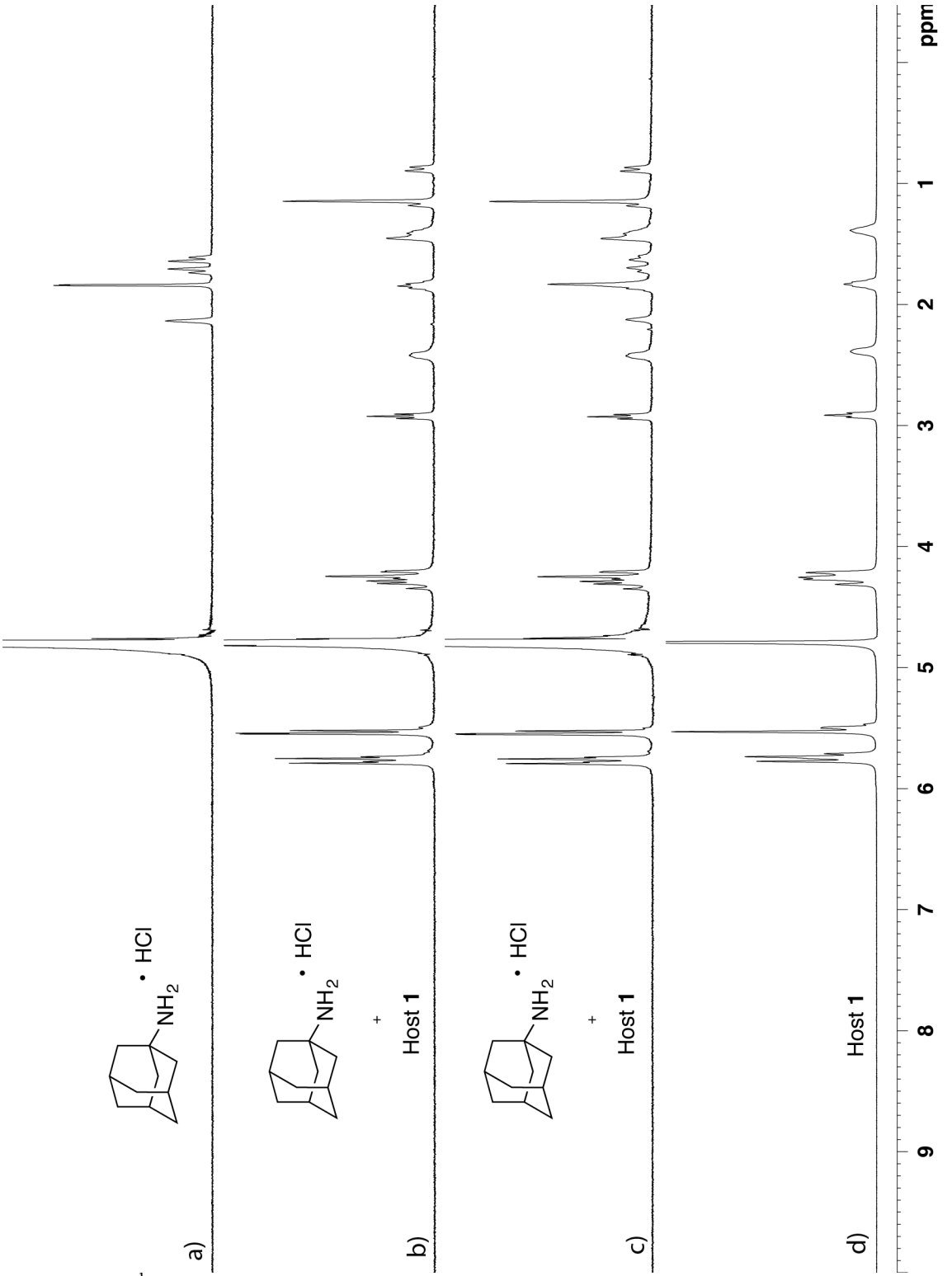

Figure S17. ^{1}H NMR spectra recorded (D_2O, 400 MHz, RT) for a) **14** (1 mM), b) a 1:1 mixture of Host **1** (1 mM) and **14** (1 mM), c) a 1:2 mixture of Host **1** (1 mM) and **14** (2 mM), d) Host **1** (1 mM).

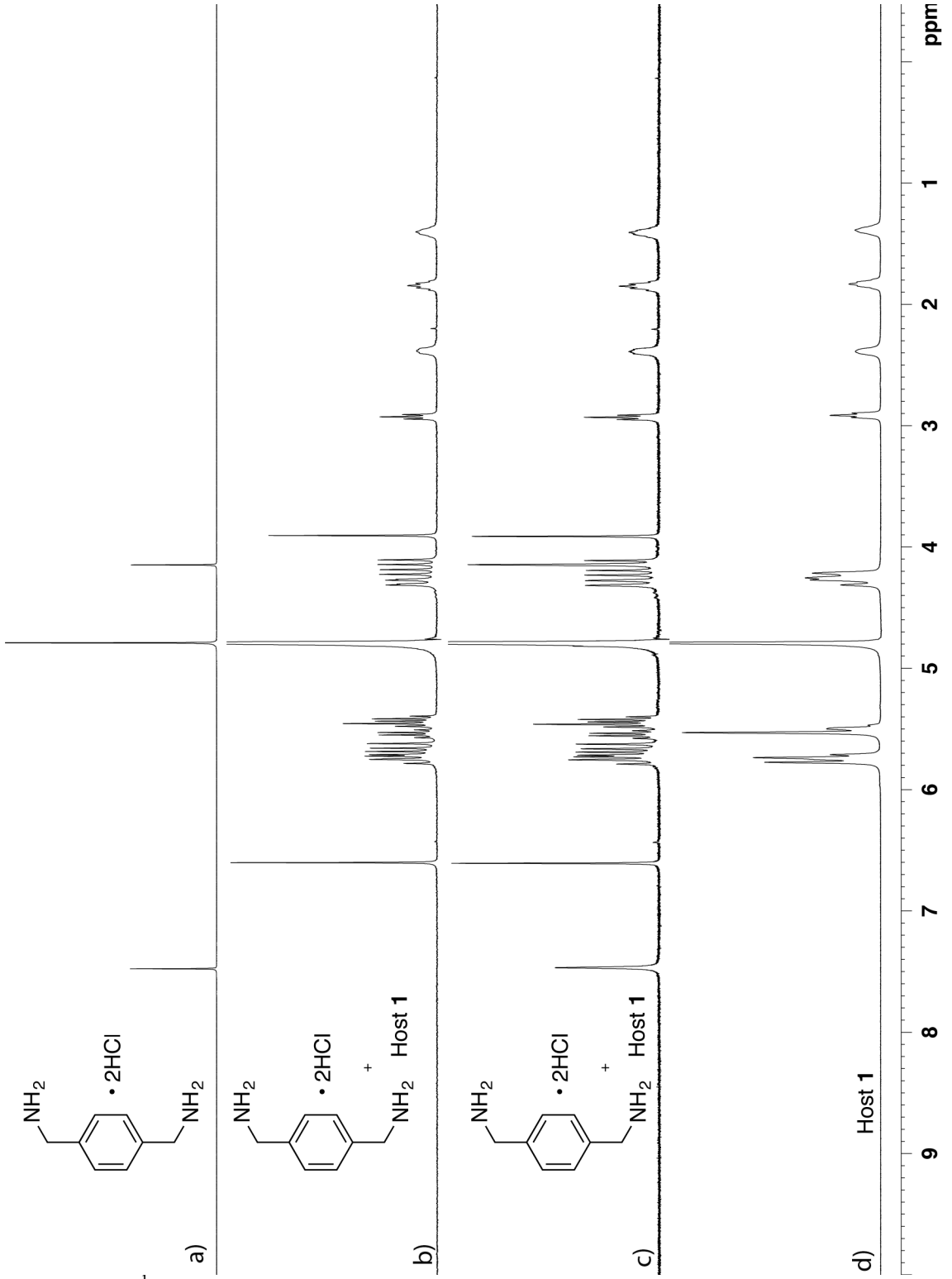

Figure S18. ^{1}H NMR spectra recorded (D_2O, 400 MHz, RT) for a) **16**, b) a 1:1 mixture of Host **1** (1 mM) and **16** (1 mM), c) a 1:2 mixture of Host **1** (1 mM) and **16** (2 mM), d) Host **1** (1 mM).

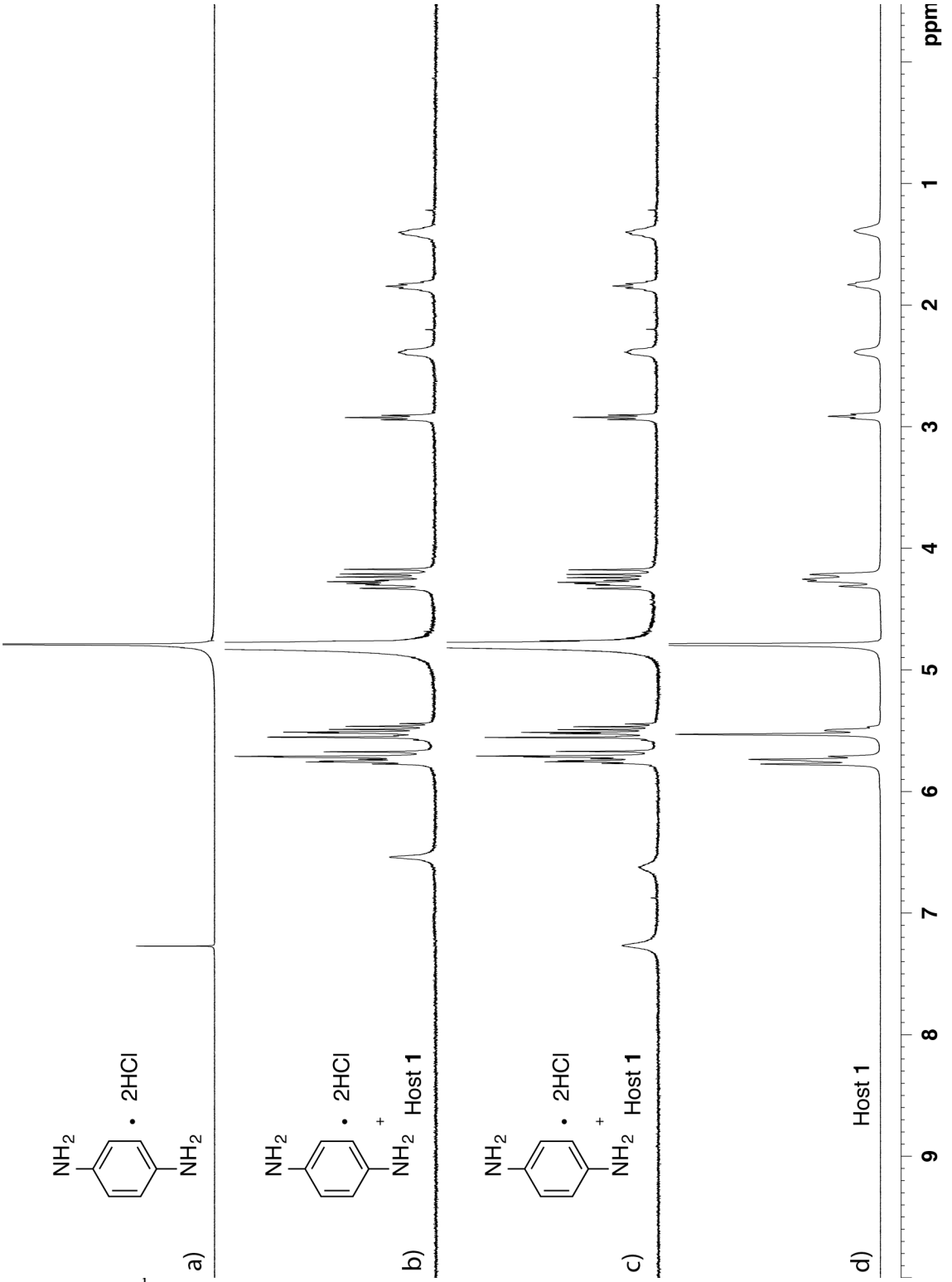

Figure S19. ^{1}H NMR spectra recorded (D_2O, 400 MHz, RT) for a) **15** (1 M), b) a 1:1 mixture of Host **1** (1 mM) and **15** (1 mM), c) a 1:2 mixture of Host **1** (1 mM) and **15** (2 mM), d) Host **1** (1 mM).

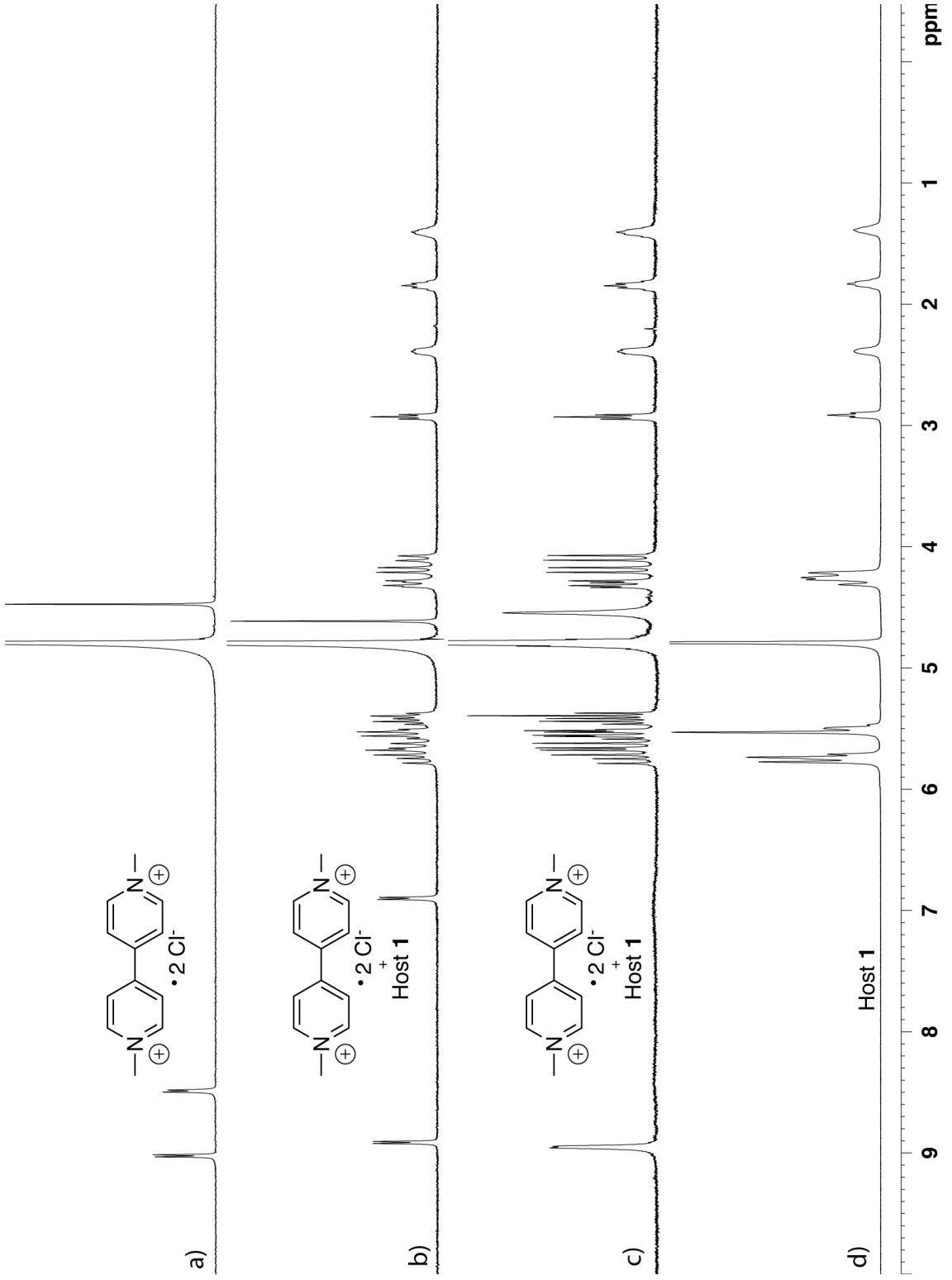

Figure S20. ^{1}H NMR spectra recorded (D_2O, 400 MHz, RT) for a) methyl viologen•2Cl$^-$ (1 mM), b) a 1:1 mixture of Host **1** (1 mM) and methyl viologen•2Cl$^-$ (1 mM), c) a 1:2 mixture of Host **1** (1 mM) and methyl viologen•2Cl$^-$ (2 mM), d) Host **1** (1 mM).

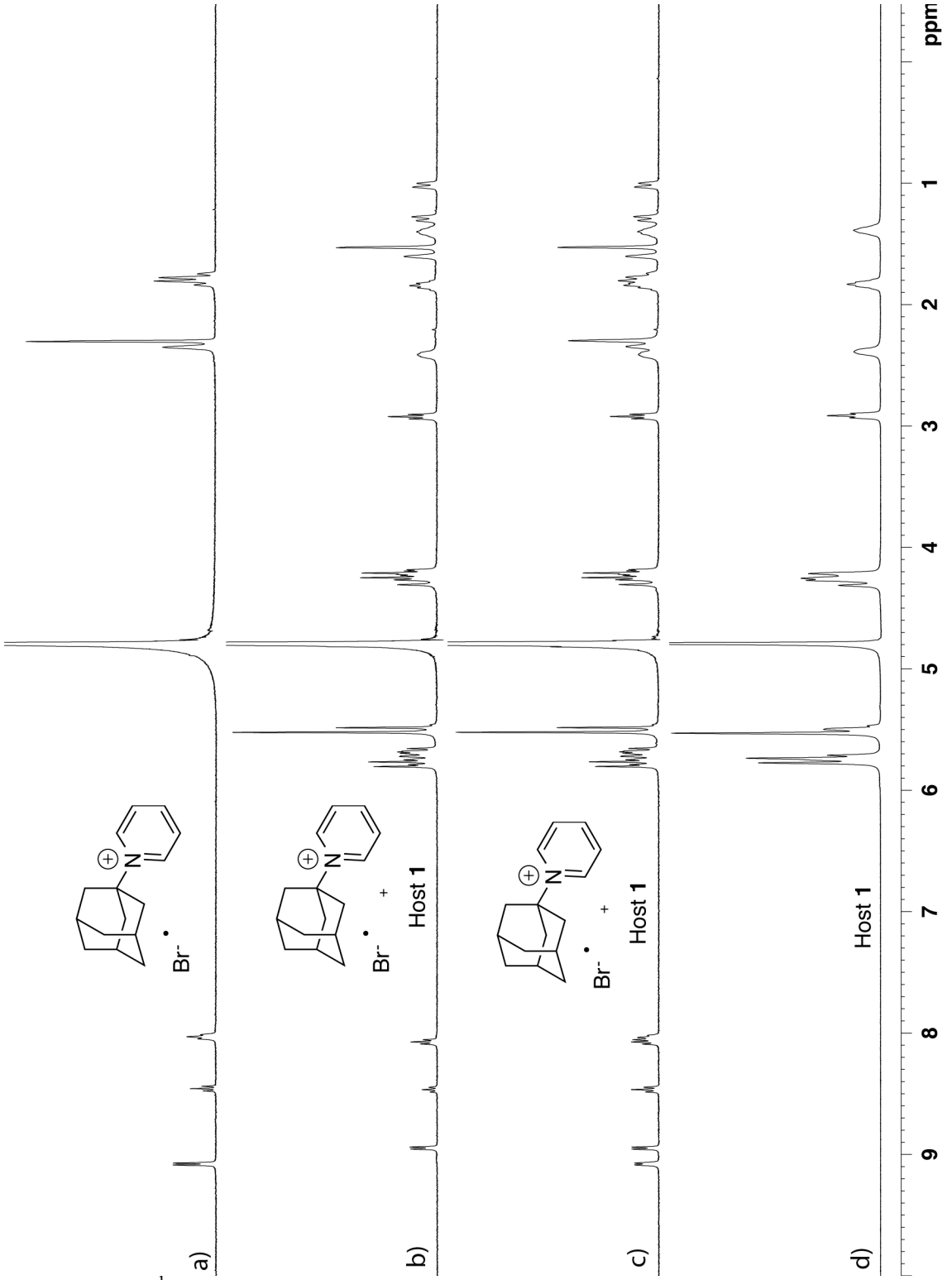

Figure S21. ^{1}H NMR spectra recorded (D_2O, 400 MHz, RT) for a) adamantyl pyridine•Br^- (1 mM), b) a 1:1 mixture of Host **1** (1 mM) and adamantyl pyridine•Br^- (1 mM), c) a 1:2 mixture of Host **1** (1 mM) and adamantyl pyridine•Br^- (2 mM), d) Host **1** (1 mM).

Procedure to measure the solubility of drugs with CB[7] and Host 1. An excess of solid drug was added to a solution of a known concentration of the host container in a 50 mM sodium sodium acetate buffer, pD = 4.74 (**18** was also tested in a 0.01 M DCl solution at pD = 2) The mixtures were stirred at room temperature for 16 h to reach equilibria. The mixtures were then centrifuged at 4400 rpm for two 10 min segments and the pellet containing the insoluble drug + drug•host complex was discarded. The supernatant was spiked with a known concentration of an internal standard (**17** and **18**: $MeSO_3H$, **12**: benzene-1,3,5-tricarboxylate sodium salt) and the concentrations of the host and drug were determined by the comparison of ^1H NMR resonance integration of the drug (**17** triplet at -0.12 ppm, **18** triplet at 1.01 ppm, **12** resonances between 6.4 and 7.7 ppm) versus the methylene/methine H-atoms of the host between 5.2 and 5.8 ppm

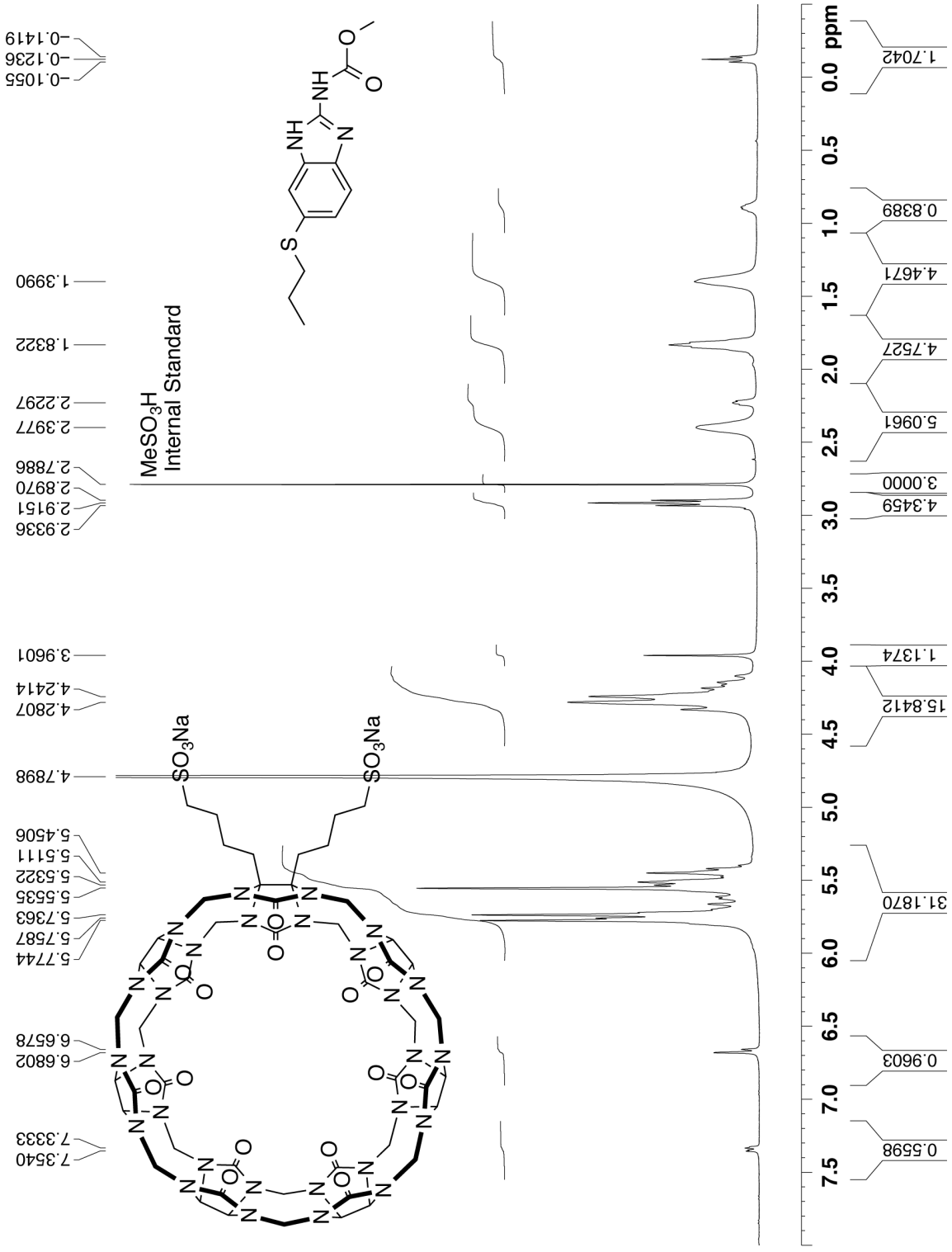

Figure S22. ^{1}H NMR spectra recorded (D_2O, 400 MHz, RT) for **17** and Host **1** using $MeSO_3H$ as an internal standard.

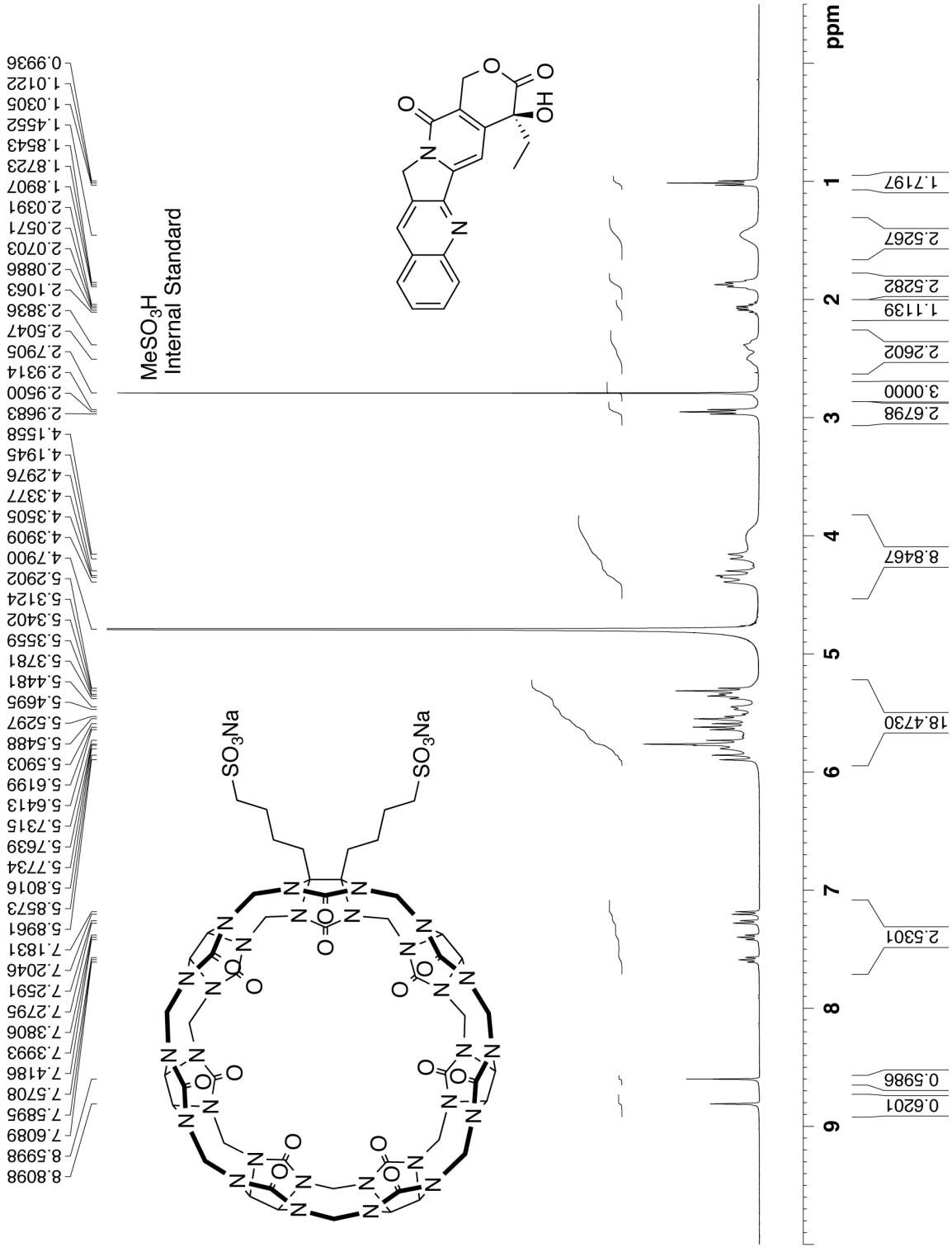

Figure S23. ^{1}H NMR spectra recorded (D_2O, 400 MHz, RT) for **18** and Host **1** using $MeSO_3H$ as an internal standard.

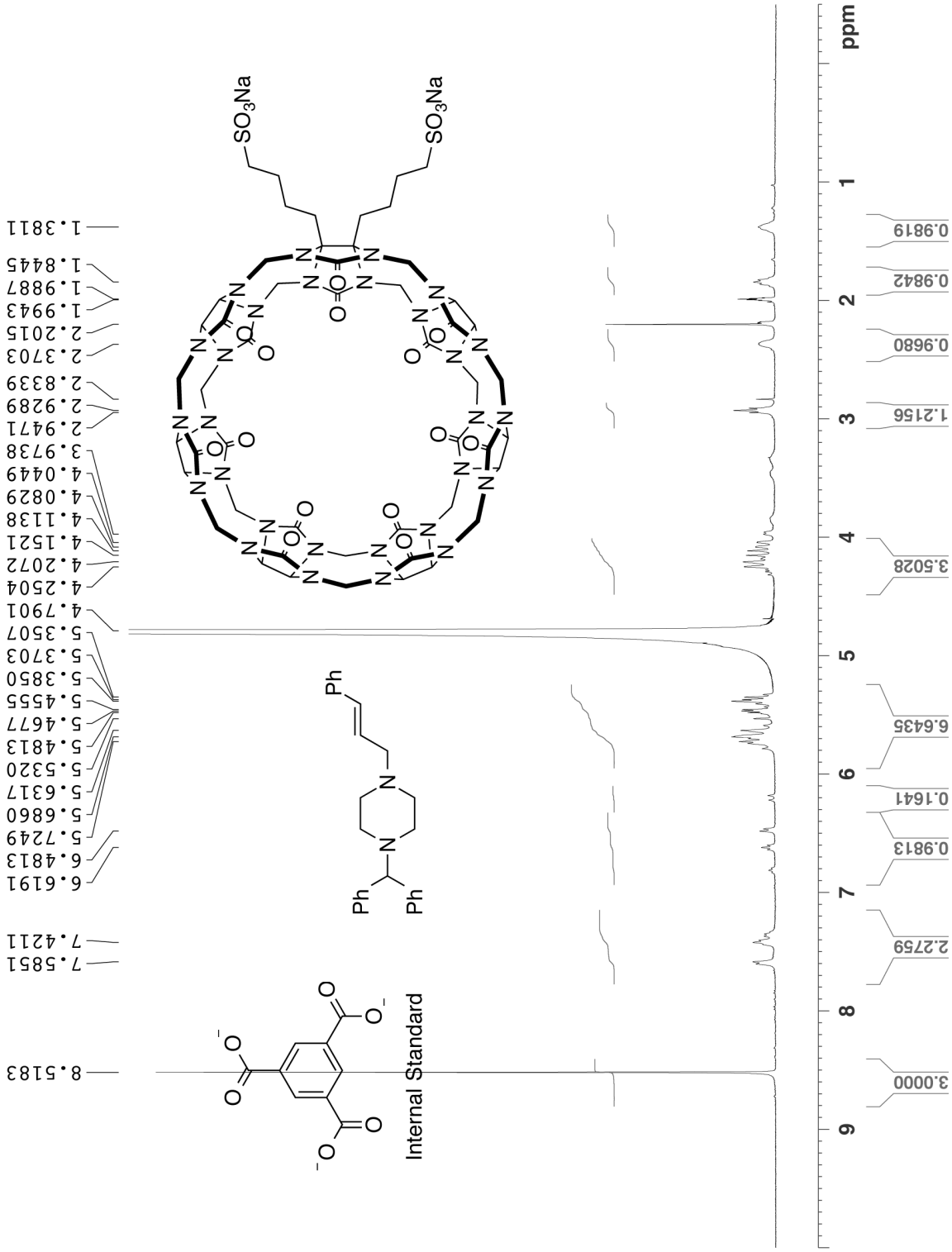

Figure S24. ^{1}H NMR spectra recorded (D_2O, 400 MHz, RT) for **12** and Host **1** using benzene-1,3,5-tricarboxylate sodium salt as an internal standard.

Phase Solubility Diagrams

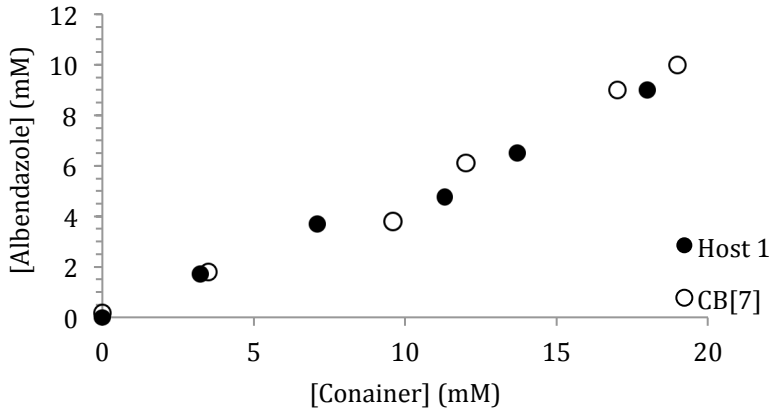

Figure S25. Phase solubility diagram for **17** with CB[7] and Host **1** (50 mM sodium acetate buffer, pD = 4.74).

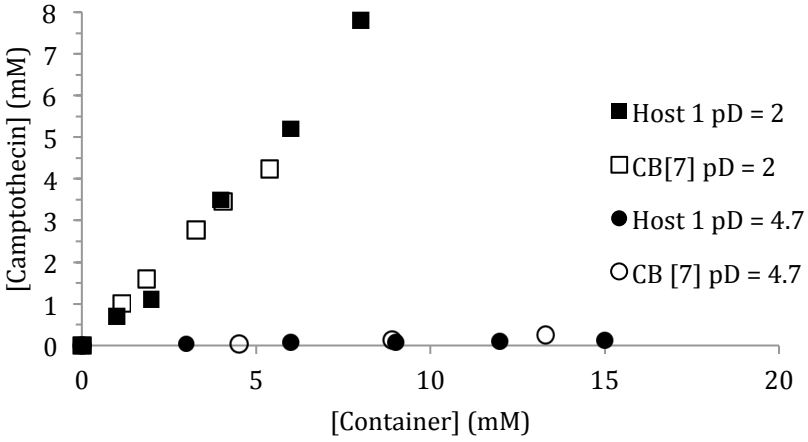

Figure S26. Phase solubility diagram for **18** with CB[7] and Host **1** (50 mM sodium acetate buffer, pD = 4.74; 0.01 mM DCl solution in D_2O, pD = 2).

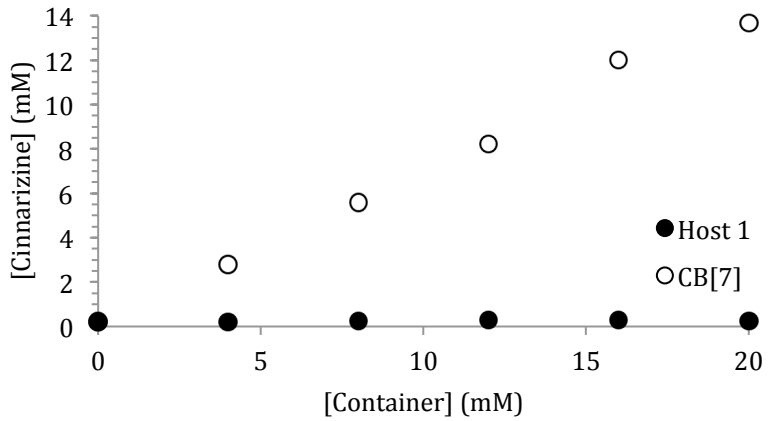

Figure S27. Phase solubility diagram for **12** with CB[7] and Host **1** (50 mM sodium acetate buffer, pD = 4.74.**1**.

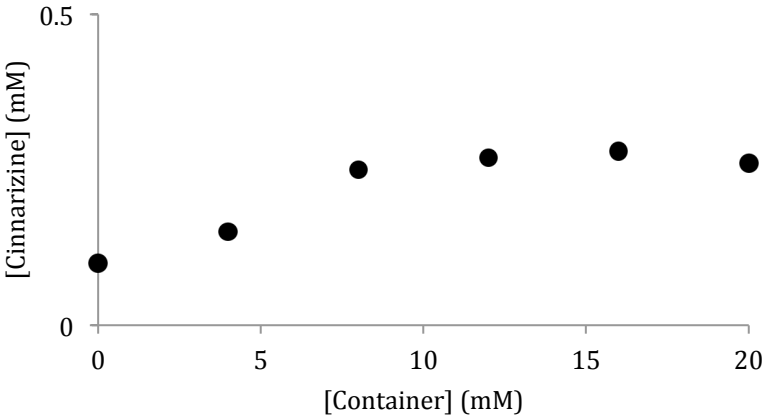

Figure S28. Phase solubility diagram for **12** and Host **1** (50 mM sodium acetate buffer, pD = 4.74).

Details of the crystal structure of Host 1

Performed by Peter Zavalij

A colorless prism-like specimen of $C_{58}H_{112}N_{30}O_{41}S_2$, approximate dimensions 0.13 mm × 0.22 mm × 0.30 mm, was used for the X-ray crystallographic analysis. The X-ray intensity data were measured on a Bruker APEX-II CCD system equipped with a graphite monochromator and a MoKα sealed tube (λ = 0.71073 Å). Data collection temperature was 150 K.

The total exposure time was 18.50 hours. The frames were integrated with the Bruker SAINT software package using a narrow-frame algorithm. The integration of the data using an orthorhombic unit cell yielded a total of 109234 reflections to a maximum θ angle of 25.00° (0.84 Å resolution), of which 30342 were independent (average redundancy 3.600, completeness = 99.9%, R_{int} = 7.13%) and 19333 (63.72%) were greater than $2\sigma(F^2)$. The final cell constants of *a* = 13.2943(11) Å, *b* = 21.6007(17) Å, *c* = 60.158(5) Å, *V* = 17275.(2) $Å^3$, are based upon the refinement of the XYZ-centroids of 9971 reflections above 20 σ(I) with 4.503° < 2θ < 40.53°. Data were corrected for absorption effects using the multi-scan method (SADABS). The calculated minimum and maximum transmission coefficients (based on crystal size) are 0.8830 and 0.9790.

The structure was solved and refined using the Bruker SHELXTL Software Package, using the space group $P2_12_12_1$, with Z = 8 for the formula unit, $C_{58}H_{112}N_{30}O_{41}S_2$. The final anisotropic full-matrix least-squares refinement on F^2 with 2098 variables converged at R_1 = 7.31%, for the observed data and wR_2 = 14.87% for all data. The goodness-of-fit was 1.002. The largest peak in the final difference electron density synthesis was 0.492 $e^-/Å^3$ and the largest hole was -0.394 $e^-/Å^3$ with an RMS

deviation of 0.059 $e^-/Å^3$. On the basis of the final model, the calculated density was 1.499 g/cm^3 and F(000), 8240 e^-.

Crystallographic References: APEX2 Version 2010.11-3 (Bruker AXS Inc.) SAINT Version 7.68A (Bruker AXS Inc., 2009) SADABS Version 2008/1 (G. M. Sheldrick, Bruker AXS Inc.) XPREP Version 2008/2 (G. M. Sheldrick, Bruker AXS Inc.) XS Version 2008/1 (G. M. Sheldrick, *Acta Cryst.* (2008). A**64**, 112-122) XL Version 2012/4 (G. M. Sheldrick, (2012) University of Gottingen, Germany) Platon (A. L. Spek, *Acta Cryst.* (1990). A**46**, C-34)

Table S1. Sample and crystal data for UM2475.

Identification code	2475	
Chemical formula	$C_{58}H_{112}N_{30}O_{41}S_2$	
Formula weight	1949.89	
Temperature	150(2) K	
Wavelength	0.71073 Å	
Crystal size	0.13 × 0.22 × 0.30 mm	
Crystal habit	colorless prism	
Crystal system	orthorhombic	
Space group	$P2_12_12_1$	
Unit cell dimensions	a = 13.2943(11) Å	α = 90°
	b = 21.6007(17) Å	β = 90°
	c = 60.158(5) Å	γ = 90°
Volume	17275.(2) $Å^3$	
Z	8	
Density (calculated)	1.499 Mg/cm^3	
Absorption coefficient	0.172 mm^{-1}	
F(000)	8240	

Table S2. Data collection and structure refinement for UM2475.

Diffractometer	Bruker APEX-II CCD
Radiation source	sealed tube, MoKα
Theta range for data collection	1.65 to 25.00°
Index ranges	$-15 \le h \le 15$, $-25 \le k \le 25$, $-71 \le l \le 71$
Reflections collected	109234
Independent reflections	30342 [R(int) = 0.0713]
Coverage of independent reflections	99.9%
Absorption correction	multi-scan

Max. and min. transmission	0.9790 and 0.8830
Structure solution technique	direct methods
Structure solution program	ShelXS-97 (Sheldrick, 2008)
Refinement method	Full-matrix least-squares on F^2
Refinement program	ShelXL-2012 (Sheldrick, 2012)
Function minimized	$\Sigma\, w(F_o^2 - F_c^2)^2$
Data / restraints / parameters	30342 / 716 / 2098
Goodness-of-fit on F^2	1.002
Δ/σ_{max}	0.001
Final R indices	19333 data; I>2σ(I) $R_1 = 0.0731$, $wR_2 = 0.1374$
	all data $R_1 = 0.1085$, $wR_2 = 0.1487$
Weighting scheme	$w=1/[\sigma^2(F_o^2)+(0.0150P)^2+31.8000P]$, $P=(F_o^2+2F_c^2)/3$
Absolute structure parameter	0.1(1)
Largest diff. peak and hole	0.492 and -0.394 eÅ^{-3}
R.M.S. deviation from mean	0.059 eÅ^{-3}

$R_{int} = \Sigma|F_o^2 - F_o^2(\text{mean})| / \Sigma[F_o^2]$
$R_1 = \Sigma||F_o| - |F_c|| / \Sigma|F_o|$
$\text{GOOF} = S = \{\Sigma[w(F_o^2 - F_c^2)^2] / (n - p)\}^{1/2}$
$wR_2 = \{\Sigma[w(F_o^2 - F_c^2)^2] / \Sigma[w(F_o^2)^2]\}^{1/2}$

Bibliography

1. Hauss, D. J. *Adv. Drug Deliv. Rev.* **2007,** *59*, 667-676.
2. Villers, A. *C. R. Fr. Acad. Sci.* **1891,** *112*, 435-438.
3. Eastburn, S. D.; Tao, B. Y. *Biotechnol. Adv.* **1994,** *12*, 325-339.
4. Buschmann, H.-J.; Schollmeyer, E. *J. .Cosmet. Sci.* **2002,** *53*, 185-191.
5. Szejtli, J. *Chem. Rev.* **1998,** *98*, 1743-1753.
6. Rekharsky, M. V.; Inoue, Y. *Chem. Rev.* **1998,** *98*, 1875-1917.
7. Guo, Q. X.; Chu, S. D.; Wang, Y. M.; Pan, Z. X.; Zhang, M. S.; Liu, Y. C. *Chin. Chem. Lett.* **1997,** *8*, 145-148.
8. Inoue, Y.; Liu, Y.; Tong, L. H.; Shen, B. J.; Jin, D. S. *J. Am. Chem. Soc.* **1993,** *115*, 10637-44.
9. Uekama, K.; Otagiri, M.; Kanie, Y.; Tanaka, S.; Ikeda, K. *Chem. Pharm. Bull.* **1975,** *23*, 1421-30.
10. Okimoto, K.; Rajewski, R. A.; Uekama, K.; Jona, J. A.; Stella, V. J. *Pharm. Res.* **1996,** *13*, 256-64.
11. Brewster, M. E.; Loftsson, T. *Adv. Drug Deliv. Rev.* **2007,** *59*, 645-666.
12. Behrend, R.; Meyer, E.; Rusche, F. *Justus Liebigs Ann. Chem.* **1905,** *339*, 1-37.
13. Freeman, W. A.; Mock, W. L.; Shih, N. Y. *J. Am. Chem. Soc.* **1981,** *103*, 7367-8.
14. Kim, J.; Jung, I.-S.; Kim, S.-Y.; Lee, E.; Kang, J.-K.; Sakamoto, S.; Yamaguchi, K.; Kim, K. *J. Am. Chem. Soc.* **2000,** *122*, 540-541.
15. Day, A.; Arnold, A. P.; Blanch, R. J.; Snushall, B. *J. Org. Chem.* **2001,** *66*, 8094-8100.
16. Liu, S.; Zavalij, P. Y.; Isaacs, L. *J. Am. Chem. Soc.* **2005,** *127*, 16798-16799.

17. Bardelang, D.; Udachin, K. A.; Leek, D. M.; Margeson, J. C.; Chan, G.; Ratcliffe, C. I.; Ripmeester, J. A. *Cryst. Growth Des.* **2011,** *11*, 5598-5614.

18. Nau, W. M.; Florea, M.; Assaf, K. I. *Isr. J. Chem.* **2011,** *51*, 559-577.

19. Koner, A. L.; Ghosh, I.; Saleh, N. i.; Nau, W. M. *Can. J. Chem.* **2011,** *89*, 139-147.

20. Liu, S.; Ruspic, C.; Mukhopadhyay, P.; Chakrabarti, S.; Zavalij, P. Y.; Isaacs, L. *J. Am. Chem. Soc.* **2005,** *127*, 15959-15967.

21. Zhao, Y.; Buck, D. P.; Morris, D. L.; Pourgholami, M. H.; Day, A. I.; Collins, J. G. *Org. Biomol. Chem.* **2008,** *6*, 4509-4515.

22. Dong, N.; Xue, S.-F.; Zhu, Q.-J.; Tao, Z.; Zhao, Y.; Yang, L.-X. *Supramol. Chem.* **2008,** *20*, 659-665.

23. Jon, S. Y.; Selvapalam, N.; Oh, D. H.; Kang, J.-K.; Kim, S.-Y.; Jeon, Y. J.; Lee, J. W.; Kim, K. *J. Am. Chem. Soc.* **2003,** *125*, 10186-10187.

24. Zhao, N.; Lloyd, G. O.; Scherman, O. A. *Chem. Commun.* **2012,** *48*, 3070-3072.

25. Lucas, D.; Minami, T.; Iannuzzi, G.; Cao, L.; Wittenberg, J. B.; Anzenbacher, P.; Isaacs, L. *J. Am. Chem. Soc.* **2011,** *133*, 17966-17976.

26. Vinciguerra, B.; Cao, L.; Cannon, J. R.; Zavalij, P. Y.; Fenselau, C.; Isaacs, L. *J. Am. Chem. Soc.* **2012,** *134*, 13133-13140.

27. Ma, D.; Hettiarachchi, G.; Nguyen, D.; Zhang, B.; Wittenberg, J. B.; Zavalij, P. Y.; Briken, V.; Isaacs, L. *Nature Chemistry* **2012,** *4*, 503-510.

28. De Kimpe, N.; D'Hondt, L.; Stanoeva, E. *Tetrahedron Lett.* **1991,** *32*, 3879-82.

29. Connors, K. A., *Binding Constants*. John Wiley & Sons: New York, 1987.